THE UNIVERSITY OF CALGARY

Analysis of GTP Variability and the Erythrocytic GTP Concentration Determining Trait (*Gtpc*) in the Mouse

by

Glenis Jane Wiebe

A THESIS

SUBMITTED TO THE FACULTY OF GRADUATE STUDIES

IN PARTIAL FULFILLMENT OF THE REQUIREMENTS FOR THE

DEGREE OF MASTER OF SCIENCE

DEPARTMENT OF BIOCHEMISTRY AND MOLECULAR BIOLOGY

CALGARY, ALBERTA

AUGUST, 1997

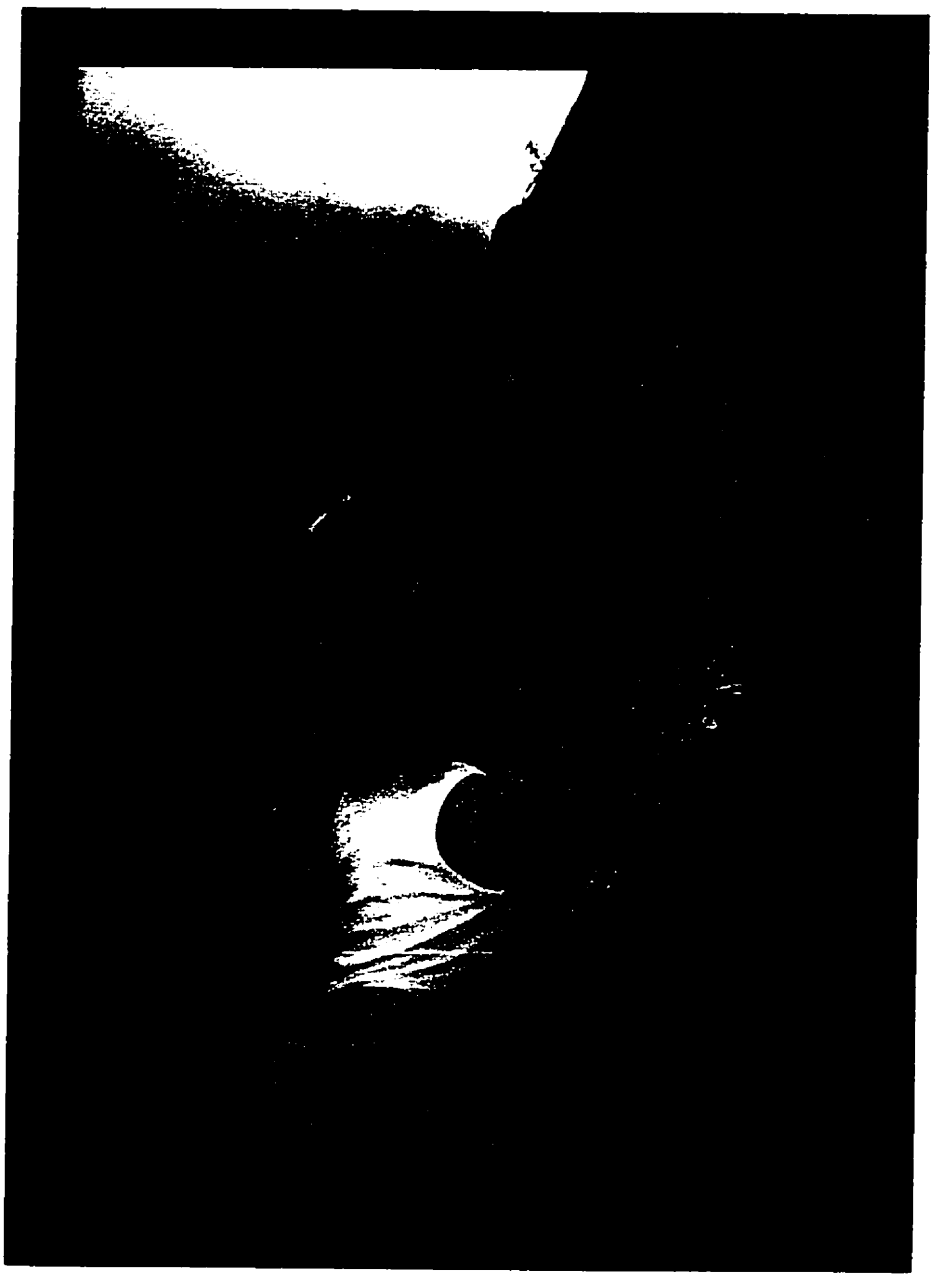

Abstract

Twenty inbred mouse strains were surveyed for erythrocytic purine nucleotide concentrations and found to segregate into two groups with respect to their GTP levels. No significant interstrain differences were observed for ATP levels. Results of nucleotide extractions from liver, kidney, heart, brain and tongue do not show any interstrain differences in GTP concentrations suggesting altered GTP levels may be a result of variations in the differentiated state of the erythrocyte. Erythrocytic GTP concentration variation was previously shown to be governed by a single gene, *Gtpc*, and linked to *Trf* on chromosome 9. Typing 232 [(B6xWB)F_1xB6] backcross progeny for *Gtpc* and eight microsatellite markers produced the following gene order and map distances: (*D9Mit14*) 0.4±0.4 (*D9Mit24*) 1.7±0.8 (*Gtpc, D9Mit51, D9Mit116, D9Mit212*) 3.9±1.3 (*D9Mit200*) 3.0±1.1 (*D9Mit20*) 7.8±1.8 (*D9Mit18*). Preliminary analysis of potential *Gtpc* gene products suggests interstrain polymorphisms of an enzyme involved in GMP degradation are responsible for the observed GTP concentration alterations.

Acknowledgements

I would like to thank my supervisor, Dr. Floyd Snyder for guidance, input, support and patience throughout this project and during the preparation of this manuscript. I would also like to thank my supervisory committee members, Dr. Torben Bech-Hansen and Dr. Fred Biddle for the advice and encouragement given along the way.
My sincerest appreciation goes to Ernest Fung for his work in the nucleotide analyses, to Dr. F. Biddle for providing the mice, and to Dr. C. Mody for supplying the human samples.

Financial support for this project was provided through an operating grant to Dr. F. Snyder from the Medical Research Council of Canada, and through Graduate Research Scholarships received from the Department of Medical Biochemistry.

Finally, I would like to express my heartfelt gratitude to my parents Drs. Leonard and Grace Wiebe for inspiring me to enter graduate studies, Cary Cuncic for sharing the experience with me, and Martin Srayko for being everything I needed: mentor, colleague and friend.

TABLE OF CONTENTS

LIST OF TABLES

List of Figures

List of Abbreviations

4AAP	4-amino-antipyrine
AXB	(A/JXC57BL/6J) RI strain
ADP	adenosine-5'-diphosphate
alamine	tri-n-octylamine
AMP	adenosine-5'-monophosphate
AMPRT	amidophosphoribosyl transferase
ATP	adenosine-5'-triphosphate
bp	base pair
BXA	(C57BL/6JXA/J) RI strain
BXD	(C57BL/6JXDBA/2J) RI strain
CAST	Cast/Ei mouse strain
CBA	CBA/FaCam mouse strain
cGMP	3',5'-cyclic GMP
cM	centiMorgan
CTP	cytosine-5'-triphosphate
dNTP	deoxyribonucleoside triphoshate
DTT	dithiothreitol
EDTA	ethylene-diaminetetra-acetic acid disodium salt
freon	trichlorotrifluoroethane
GD	guanine deaminase

GDP	guanosine-5'-diphosphate
GMP	guanosine-5'-monophosphate
GTP	guanosine-5'-triphosphate
Gtpc	mouse erythrocytic GTP concentration determining trait
HGPRT	hypoxanthine-guanine phosphoribosyl transferase
HPLC	high-performance liquid chromatography
IMP	inosine-5'-monophosphate
IMPDH	IMP dehydrogenase
M.	*Mus*
MGD	Mouse Genome Database, Jackson Laboratories
MIT	the MIT Center for Genome Research
NAD	nicotinamide adenine dinucleotide
NT	5'-nucleotidase
OB	C57Bl/6J-ob/ob mouse strain
PCR	polymerase chain reaction
PNP	purine nucleoside phosphorylase
POD	peroxidase
PP-ribose-P	5-phosphoribosyl-α-1-pyrophosphate
RBCs	red blood cells
RFLP	restriction fragment length polymorphism
SDP	strain distribution pattern

SDS	sodium dodecyl sulfate
S.E.	standard error
SSLP	simple sequence length polymorphism
SSR	simple sequence repeat
TBHB	2,4,6-tribromo-3-hydroxybenzoic acid
Trf	mouse transferrin gene
Tris	tris-(hydroxymethyl)-aminomethane
TTP	thimidine-5'-triphosphate
UOX	uricase
UTP	uridine-5'-triphosphate
WB	WB/ReJ mouse strain
XMP	xanthosine-5'-monophosphate
XO	xanthine oxidase
YAC	yeast artificial chromosome

INTRODUCTION

Guanosine-5'-Triphosphate

Guanosine-5'-triphosphate (GTP) is a purine nucleotide involved in many important cellular functions, such as energy metabolism, signal transduction, and cell proliferation. As a substrate, GTP is used in RNA production, as well as in the *de novo* synthesis of the pterin co-factor tetrahydrobiopterin. As an energy source, GTP is utilized in protein synthesis by initiation factor eIF2, elongation factors EF1 and EF2 (also known as a translocation factor) and release factor RF1. GTP also provides the high-energy phosphate bond required by phosphoenol-pyruvate carboxykinase in gluconeogenesis, a function carried out primarily by the liver to provide glucose to the organism. Gluconeogenesis is especially important during periods of starvation and intense exercise when blood glucose levels drop dramatically.

Cellular signal transduction via G-proteins occurs through the binding and hydrolysis of GTP and subsequent interactions with effector molecules (Bourne *et al.* 1990, 1991). The enzyme guanylate cyclase catalyzes the conversion of GTP to 3', 5'-cyclic GMP (cGMP). cGMP either acts directly on target molecules or activates cGMP protein kinases,

which in turn activate other molecules through phosphorylation, resulting in a variety of metabolic changes.

The rate of *de novo* GTP synthesis displays a positive correlation with cellular proliferation rates (Willis & Seegmiller 1980). A more than 2-fold increase in GTP has been observed in dividing *versus* non-dividing lymphoblasts (Gruber *et al.* 1985). In addition, a marked expansion of the cellular GTP pool is observed preceding the onset of exponential growth in hepatoma cells (Weber *et al.* 1981). Furthermore, GTP levels appear to be regulated, at least in part, by the p53 gene product, which influences the G1 to S phase cell cycle transition (Sherley 1991).

Microtubule assembly and glycoprotein production are two further examples of where GTP is required. Microtubules are involved in many architectural and contractile cell functions, and are formed by GTP-mediated tubulin assembly and disassembly (Kirschner & Mitchison 1986). Glycoproteins function in intercellular recognition and act as receptors on the outer surface of many cells or as degradation enzymes within lysosomes. Mannose and its derivatives are incorporated into complex polysaccharides on glycoproteins by way of GDP-mannose, which is made from mannose-1-phosphate and GTP.

GTP Synthesis

Three different routes are used for GTP production in the cell. The primary source of GTP is the *de novo* purine metabolic pathway (Figure 1). This pathway uses non-purine precursors to form the purine ring. The first point of regulation occurs at the first committed step in the purine biosynthesis pathway: the condensation of L-glutamine and 5-phosphoribosyl-α-1-pyrophosphate (PP-ribose-P) by amidophosphoribosyl transferase (AMPRT) to form 5-phospho-β-D-ribosylamine. This reaction is activated by increased levels of PP-ribose-P and inhibited by the pathway end-products, namely purine ribonucleotides.

The second point of regulation occurs at the inosine-5'-monophosphate (IMP) branchpoint leading to either guanine or adenine nucleotide production. The rate-limiting step in guanine nucleotide synthesis is catalyzed by IMP dehydrogenase (IMPDH), which is negatively affected by guanosine-5'-monophosphate (GMP). Adenylosuccinate synthase is the corresponding enzyme in the adenine nucleotide arm of the purine metabolic pathway. This step is dependent upon the abundance of guanine nucleotides in the cell, as it requires GTP to catalyze the reaction.

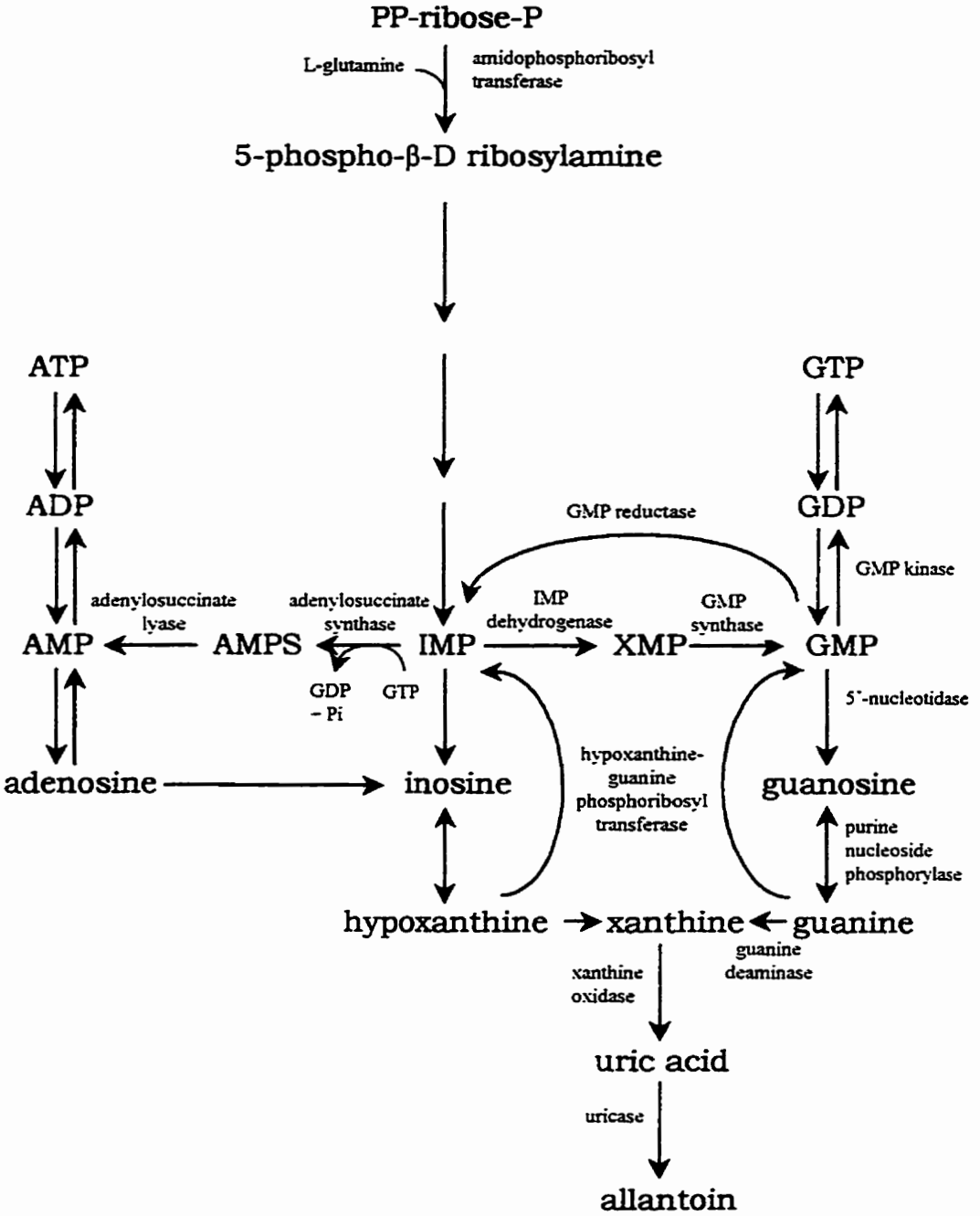

Figure 1. The purine metabolic pathway.

An alternate route for the synthesis of GTP is through the salvage pathway from the preformed guanine or hypoxanthine bases obtained through dietary sources, or from nucleotide turnover. The first step in this pathway is catalyzed by hypoxanthine-guanine phosphoribosyl transferase (HGPRT). As with *de novo* synthesis, the salvage pathway is also inhibited by GMP.

Finally, GTP is also formed from guanosine-5'-diphosphate (GDP) by succinate thiokinase in the tricarboxylic acid cycle, which functions in the oxidation of amino acids, fatty acids and carbohydrates and provides intermediates to other biosynthetic pathways.

GTP Degradation

The degradation pathway features four enzymes. GMP reductase, 5'- nucleotidase, purine nucleoside phosphorylase (PNP) and guanine deaminase function specifically in the degradation of guanine nucleotides. GMP reductase facilitates the formation of IMP from GMP. The 5'-nucleotidase plays a role in the catabolism of GMP to guanosine, the latter of which can be removed from the cell via nucleoside transporters. PNP catalyzes the reversible breakdown of guanosine to guanine, whereas guanine deaminase converts guanine into xanthine in

an irreversible step. The products of each of these reactions can leave the cell through facilitated diffusion.

The degradation product of GTP in humans is ultimately uric acid, which is excreted by the kidneys. Disorders of the purine metabolic pathway such as a complete or partial deficiency of HGPRT can result in an excess of uric acid, also known as hyperuricemia, which can lead to gout and renal disease. In non-primate mammals, uric acid is catabolized to allantoin by the liver.

GTP-Associated Neurological Disorders

Several neurological disorders are recognized to be associated with reduced erythrocytic GTP levels or impaired utilization of GTP. For example, erythrocytic GTP concentrations are reduced as much as 75% in patients with Lesch Nyhan syndrome, which results from a complete deficiency in HGPRT (Seegmiller *et al.* 1967). Those afflicted show moderate mental retardation, spasticity and choreoathetosis, as well as a propensity toward self-injurious behaviour such as biting lips or fingertips, or banging their heads against nearby objects (Lesch & Nyhan 1964). Purine nucleoside phosphorylase deficiency results in a 10% reduction of erythrocytic GTP levels and has accompanying cellular

immunity defects, as well as behavioural abnormalities and spasticity (Simmonds *et al.* 1988). More recently, a partial defect in GTP cyclohydrolase I has been associated with hereditary progressive dystonia, the phenotype of which includes dystonic or abnormal posturing with characteristic diurnal fluctuations (Ichinose *et al.* 1994). GTP cyclohydrolase I uses GTP as a substrate and catalyzes the rate limiting step in the *de novo* synthesis of the pterin cofactor tetrahydrobiopterin (Nichol *et al.* 1985), which is essential in the production of the neurotransmitter, dopamine. The neurological abnormalities associated with HGPRT and PNP deficiencies may also arise as a result of a reduction of GTP utilization or availability in neurotransmitter production. This would, however, require that GTP levels were reduced in the central nervous system as well as in the erythrocytes of patients; the former has not been determined (Simmonds *et al.* 1987).

Interestingly, mouse models of the above enzymatic deficiencies, show none of the associated neurological disorders (Kuehn *et al.* 1987; Snyder *et al.* 1994; McDonald *et al.* 1988). The reason for this is unknown, but may be due to differences in GTP requirements for normal neuronal development and function, and/or differences between mice and humans in GTP metabolism and regulation. Understanding these

differences may be important for developing therapies to compensate for enzymatic deficiencies in purine metabolism in humans.

GTP Variability in the Mouse

The assessment of erythrocytic nucleotide pools in the mouse led to the discovery that the concentration of GTP differs among phenotypically normal inbred mouse strains by as much as 10-14 fold (Henderson *et al.* 1983), suggesting the presence of an enzymatic polymorphism that influences the levels of erythrocytic GTP. Comparative studies of five enzymes involved in purine metabolism, HGPRT, adenine phosphoribosyl transferase, adenosine deaminase, guanine deaminase, and adenosine kinase, were performed by Henderson *et al.* (1983) in an attempt to explain these differences. Although enzyme activities and rates of metabolism differed between strains, the variations did not correlate with observed erythrocytic nucleotide content.

Since distinguishable phenotypes may be used as markers to genetically map a given locus through linkage analysis, the heterogeneity of mouse erythrocytic GTP levels was subsequently studied in the laboratory of Dr. F. F. Snyder using a genetic approach. A survey of

erythrocytic GTP pools in nine laboratory mouse strains carried out by Jenuth *et al.* (1994) revealed that the differing concentrations could be divided into two distinct groups: strains with low GTP levels (C3H/HeJ, C3H/HeHa, A/J, and WB/ReJ) and strains with high GTP levels (AKR/J, DBA/2J, CBA/J, C57BL/6J, and C57L/J). No significant variation in interstrain adenosine-5'-triphosphate (ATP) levels was observed. Offspring of crosses between mice from high GTP strains and low GTP strains were found to exhibit intermediate GTP levels. Backcrosses of the F_1's with parental strains resulted in individuals that segregated into F_1-like or parental-like GTP concentrations in a 1:1 ratio. These findings suggested that the GTP concentration determining trait was governed by a single locus, subsequently designated *Gtpc*, and was inherited in an autosomal co-dominant manner. Analysis of GTP levels within the C57BL/6JXC3H/HeJ (BXH) recombinant inbred strain set, followed by strain distribution pattern comparisons pointed to possible linkage of *Gtpc* with loci on either chromosome 5 or 9.

Using [(CBA/JXWB/ReJ)F_1XWB/ReJ] backcross analysis, a recombination frequency of 14.6±5.5 cM (n=41) was observed between transferrin (*Trf*) and *Gtpc* confirming its position on mouse chromosome 9 (Snyder *et al.* 1995; unpublished results). Preliminary linkage analysis using microsatellite markers *D9Mit10*, *D9Mit35*, *D9Mit12*, and *D9Mit14*, showed *Gtpc* to be located on the telomeric side of *Trf*.

The work presented here was undertaken to investigate the GTP concentration variability among mouse strains, to address tissue specificity, to refine the map position of *Gtpc*, and to assess candidate gene products. To examine the extent of variability within this trait, an extensive survey of mouse purine nucleotide levels was carried out. Included in this survey were 18 laboratory inbred strains (which arise from *Mus musculus domesticus* and *Mus musculus musculus* progenitors), a wild strain of *Mus musculus domesticus*, the subspecies *Mus musculus castaneus* and the separate species, *Mus spretus*. Also included is a study of human erythrocytic purine nucleotide concentrations, which was carried out to determine if the GTP variability observed in mouse erythrocytes could also be detected in a sample of the normal human population.

Nucleotide levels were measured in other cells and tissues in order to ascertain whether the GTP concentration variability observed between strains is a feature restricted to erythrocytes, or whether this phenomenon is observed in other cells as well. Preliminary studies by Snyder *et al.* (1994) indicated no GTP concentration differences in spleen leukocytes.

The map position of *Gtpc* was refined by backcross analysis using microsatellite markers. The [(CBA/JxWB/ReJ)F_1xWB/ReJ] backcross used by Snyder *et al.* (1994) was not as informative as desired for regions

distal to *Trf*. Since C57BL/6J (B6) and WB/ReJ (WB) exhibit useful repeat length polymorphisms in this region, a [(B6xWB)F_1xB6] backcross was set up to localize *Gtpc*. Recombinant inbred strains, A/JXC57BL/6J (AXB), C57BL/6JXA/J (BXA), C57BL/6JXDBA/2J (BXD), and C57BL/6JXC3H/HeJ (BXH), were typed with microsatellite markers informative for *Gtpc* mapping, as a means of obtaining further information with respect to the distal region of mouse chromosome 9.

Finally, some preliminary work was undertaken to assess gene products for identity with *Gtpc*, *i.e.* whether they could be responsible for the observed GTP differences. Candidates considered included those known to be involved in GTP utilization or production. Particular interest was placed upon enzymes known to function in the guanine nucleotide metabolic pathway.

Materials and Methods

Measuring Erythrocytic Purine Nucleotide Levels in Inbred Mouse Strains

For erythrocytic nucleotide pool determination, strains were chosen based on in-house accessibility to represent a cross section of laboratory inbred strains derived from *Mus musculus musculus* and *Mus musculus domesticus* progenitors. Additionally, *Mus spretus*, *Mus musculus castaneus* and PERU W1-II (*Mus musculus domesticus*) were sampled in order to determine whether nucleotides vary between different species or subspecies. The majority of inbred mouse strains were obtained from F. G. Biddle (University of Calgary), which have been previously described by Biddle & Eales (1996) and Biddle *et al.* (1993). The B6-NPF strain, reported by Mably *et al.* (1989), Jenuth *et al.* (1991), and Snyder *et al.* (1994), is maintained by F. F. Snyder (University of Calgary). CD-1 mice were imported from Charles River.

Erythrocytic nucleotides were extracted by a trichloroacetic acid/alamine-freon method as previously described (Jenuth *et al.* 1994). Blood samples were obtained via the orbital sinus of the mice using heparinized microhematocrit capillary tubes (Snyder *et al.* 1994). Briefly, erythrocytes were pelleted by centrifugation at 2500*g* for 1 minute at room temperature. A 0.1 mL packed cell volume was then extracted with

2.5 volumes of 12% trichloroacetic acid (TCA) at 4°C, and centrifuged at 14,000*g* for 1 minute at room temperature. The supernatant was removed and neutralized with 0.5 M tri-n-octylamine (alamine) in 1,1,2-trichlorotrifluoroethane (freon) using bromophenol blue as pH indicator. The aqueous layer was then removed and stored at -20°C until analyzed.

Nucleotides were separated from these samples on a SpectraSYSTEM liquid chromatograph (Thermo Separation Products, San Jose, CA) using a 4.6 x 250 mm PartiSphere-5-SAX column (Whatman, NJ). The SpectraSYSTEM consisted of an SCM400 degasser, P4000 solvent delivery system, AS3000 autosampler, a scanning SpectraFocus detector, and PC1000 operating system software. The starting buffer (A) was 10 mM potassium phosphate pH 3.5 and the second buffer (B) was 1 M potassium phosphate. The autosampler and column temperature was maintained at 5°C and 30°C respectively. The flow rate was 1 mL/minute. The column was initially equilibrated with 100% buffer A for 20 minutes before injection of 0.01 mL of sample. The mobile phase schedule was 100% buffer A from 0 to 5 minutes, followed by a linear gradient attaining 70% buffer B at 25 minutes, unchanged to 40 minutes, and then a linear gradient to 100% buffer A at 50 minutes. The detector was set to scan from 200 to 300 nm at 5 nm interval at a rate of 11.52 Hz. A signal at 255 nm was used for quantitation. Nucleotides were identified by retention times and further verified by

their absorption spectra. The concentration of each nucleotide was determined by the integration of the area underneath the absorbance peak and comparison to a known concentration of the same compound. Since samples originated from packed cells, concentrations were then converted into units of nmol/mL packed cells.

Determining GTP Concentrations in Nucleated Tissues

GTP concentrations in tissues other than erythrocytes were determined following a protocol based on methods by Cross *et al.* (1993), Perrett & Grune (1994), and Bøtker *et al.* (1994). To ensure minimal nucleotide degradation prior to extraction, mice were anaesthetized with 0.3 mL per 10 g body weight of a 1.25% tribromoethanol solution (2:1 weight/weight 2,2,2-tribromoethanol:amylene hydrate (*T*-amyl alcohol)) (Cunliffe-Beamer 1983). After tissues were removed, mice were sacrificed by cervical dislocation. Small amounts of tissue, approximating 0.1 g, were immediately homogenized at 4°C in 2-3X volume/weight 12% trichloroacetic acid, and centrifuged at 2500*g* for 10 minutes at 4°C. The supernatant was neutralized, and nucleotides from the tissue extracts were separated by high-performance liquid chromatography (HPLC) as outlined for erythrocyte-based samples.

Mapping the Erythrocytic GTP Concentration Determining Trait (Gtpc) on Mouse Chromosome 9

C57BL/6J (B6) females were crossed to WB/ReJ (WB) male mice. The resulting F_1 offspring were subsequently backcrossed to B6 mice. Seven backcrosses in total were set up: two in which the F_1 parent was male, and five in which the F_1 parent was female (Table 1). Two-hundred-and-thirty-two backcross offspring were used to map the position of *Gtpc*. Standard mating notation places the female parent before the male. Therefore, backcrosses would be [(B6XWB)F_1XB6] or [B6X(B6XWB)F_1] depending on the direction of the cross. However, since all data are pooled, the notation [(B6XWB)F_1XB6] will be used to refer to the total population.

DNA was extracted from 1 cm tail clippings using a modified procedure of Laird *et al.* (1991). The tissues were incubated in 0.5 mL lysis mixture (100 mM Tris-HCl pH 8.5, 5 mM EDTA, 0.2% SDS, 200 mM NaCl, 200 µg/mL proteinase K) overnight at 55°C. Following gentle mixing, samples were centrifuged for 10 minutes at 14,000*g* at room temperature. The supernatant was collected, and the DNA was precipitated with an equal volume of isopropanol. DNA was then transferred to a new tube and dissolved in 0.5 mL sterile ddH_2O for 4-6 hours at 55°C with gentle periodic mixing. Absorbance readings at 260

nm were used for quantitation, and absorbance ratios of 260 nm/280 nm were used to monitor the purity of the DNA samples. A pure preparation of DNA has a 260 nm/280 nm value of 1.8; lower values indicate protein contamination. Ratios obtained using this extraction method typically ranged from 1.4 to 1.8.

Table 1. Summary of backcrosses used to map *Gtpc*.

Backcross	**Male Offspring**	**Female Offspring**
B6 female X F_1 male (A)	11	6
B6 female X F_1 male (B)	1	6
F_1 female X B6 male (C)	24	27
F_1 female X B6 male (D)	48*	43*
F_1 female X B6 male (E)	48*	43*
F_1 female X B6 male (F)	24	30
F_1 female X B6 male (G)	5	7

Note: F_1's are the offspring of a (B6XWB) cross.

* The offspring numbers given are for crosses D & E as these were housed together.

Polymerase chain reaction (PCR) analysis was carried out in 50 µL reaction volumes containing 1X PCR buffer (BRL) (20 mM Tris-HCl pH 8.4, 50 mM KCl), 0.2 mM dNTPs (Boehringer Mannheim), 1-2 mM $MgCl_2$ (BRL) as necessary for optimal results, 0.26 µM forward and reverse primers, 0.5-1µg DNA, and 2U Taq polymerase (BRL). Primer pairs used were *D9Mit14*, *D9Mit18*, *D9Mit20*, *D9Mit24*, *D9Mit51*, *D9Mit116*, *D9Mit200*, and *D9Mit212* (Research Genetics).

Samples were amplified on a Perkin-Elmer Cetus DNA Thermal Cycler with an initial incubation at 94°C for 6 minutes, 35 cycles of 1 minute at 94°C, 1 minute at 55°C, and 1 minute at 72°C, and a final extension at 72°C for 7 minutes. Marker dye was added to a 1X final concentration (10% v/v glycerol, 0.2% bromophenol blue, 1X TBE), and 10 µL of the product was then subjected to electrophoresis on 4% agarose gel in 1X TBE (100 mM Tris, 100 mM boric acid, 1 mM EDTA). DNA molecular weight marker V (HaeIII cleaved pBR322 DNA) (Boehringer Mannheim) was included as a size standard. Gels were electrophoresed at 75 mA limiting conditions for 45 minutes in the presence of ethidium bromide (0.25 µg/mL), and photographed using short-wave ultraviolet and type 52 Polaroid film.

The genotype for the GTP concentration determining trait, *Gtpc*, was inferred by the phenotypic assessment of erythrocytic GTP levels. For each [(B6XWB)F_1XB6] backcross offspring, GTP concentrations were

determined to be high (parental or B6-like) or intermediate (F_1-like) using the nucleotide extraction/analysis method outlined earlier. DNA from individual mice were then typed using microsatellite markers polymorphic for B6 and WB, to determine whether they were B6-like or F_1-like with respect to amplification products.

Recombination events were recorded between *Gtpc* and microsatellite markers, as well as between the markers themselves. The percentage of individuals in which recombination between two markers has occurred corresponds to the distance between the two markers in centiMorgans (cM). Gene order was established using calculated distances for each marker both with respect to all other markers and to *Gtpc*.

Mapping the Gtpc-Informative Microsatellite Markers in Recombinant Inbred Strains

Microsatellite amplification in AXB, BXA, BXD and BXH recombinant inbred (RI) strains was carried out as outlined for backcross analysis. RI strain DNA was purchased from Jackson Laboratories. A strain distribution pattern (SDP) for each RI set was produced by comparing the length of the amplification product for each strain within

the set to the appropriate parental strain, then designating each as being either of one parental-type or the other. For example, each strain within the BXH RI strain set is designated as either B or H.

Assessing Candidate Gene Products for Identity with Gtpc

Blood samples were obtained via the orbital sinus of B6 or WB mice, as previously described for erythrocytic nucleotide extractions. Samples were centrifuged at 2500*g* for 1 minute at room temperature. Pelleted red blood cells (RBCs) were removed, washed twice in 0.9% (physiological) saline, and frozen at -20°C until use.

RBCs were thawed and diluted with an equal volume of 100 mM Tris-HCl pH 7.5. Samples were vortexed, subjected to two freeze-thaw cycles, and centrifuged at 2500*g* for 15 minutes at 4°C. The supernatant was diluted 5-fold in ddH_2O, and 3 mg activated charcoal was added to remove endogenous nucleotides (Torres *et al.* 1994). Samples were then vortexed, allowed to stand on ice for 15 minutes with occasional mixing, and finally centrifuged as before. The supernatant was removed and placed on ice for immediate use, or aliquoted and stored at -20°C. Protein concentrations were determined using colourimetric assays (BioRad) based on the Bradford dye-binding procedure (Bradford 1976).

Two different assay methods, using either high performance liquid chromatographic (HPLC) or spectrophotometric analysis were employed to look at the utilization of different substrates in the purine metabolic pathway. The first assay employed an approach modified from Alexiou and Leese (1994). Reactions were carried out in 0.1 mL volumes containing 50 mM Tris-HCl pH 7.4, 2.5 mM $MgCl_2$, 0.25 mM DTT with GMP or GTP as a substrate. When using IMP as a substrate, 0.1 mL reaction mixtures contained 100 mM Tris-HCl pH 8.0, 0.1 M KCl, 3 mM EDTA, 0.5 mM NAD (Hodges *et al.* 1989). Each sample contained 0.5 mM of the respective substrate, and approximately 9 mg/mL of B6 or WB RBC lysates. After addition of the substrate, samples were incubated at 37°C for 0, 5, 20 and 60 minutes. The reactions were stopped by adding 20 µL 50% TCA. Samples were then processed and analyzed as for the nucleotide extractions.

The second assay was modified from a procedure by LeTissier *et al.* (1994). Reactions were carried out in 5 mM phosphate buffer pH 7.4, 50 mM Tris-HCl pH 7.6, 1 mM TBHB (2,4,6-tribromo-3-hydroxybenzoic acid), 0.1 mM 4AAP (4-amino-antipyrine), 3 U/mL peroxidase, 0.040 U/mL xanthine oxidase, 0.015 U/mL uricase. Each sample contained 0.5 mM of substrate, either guanosine or GMP, and 0.5 mg/mL protein. After addition of the substrate, samples were incubated at 37°C and the increase in absorbance at 512 nm was measured over a period of 30

minutes. One unit change in absorbance is equivalent to the conversion of 7.4 nmol of substrate (LeTissier *et al.* 1994). Refer to Figure 2 for a summary of the principles pertinent to this assay method.

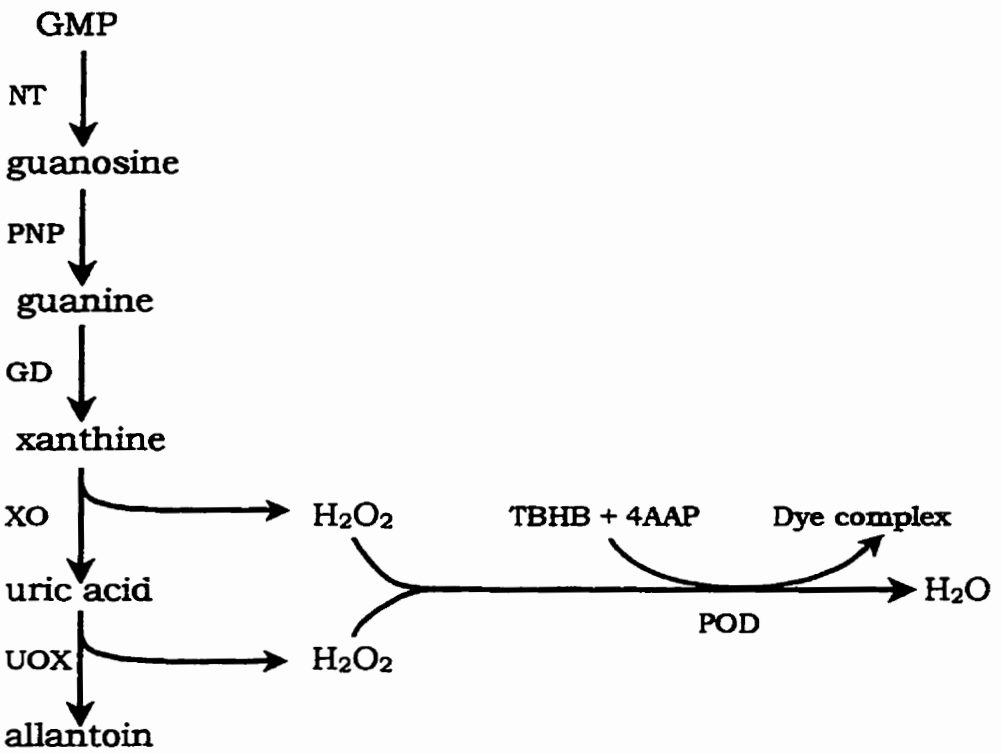

Figure 2. The basic principle of the spectrophotometric assay used to evaluate GMP and guanosine degradation. Abbreviations used are NT - 5'-nucleotidase, PNP - purine nucleoside phosphorylase, GD - guanine deaminase, XO - xanthine oxidase, UOX - uricase, POD - peroxidase, TBHB - 2,4,6-tribromo-3-hydroxybenzoic acid, 4AAP - 4-amino-antipyrine. Dye complex formation is measured at 512 nm.

Data Analyses

Scheffé's, Student-Newman-Keuls and Rankit statistical analyses of GTP and ATP concentrations, and GTP/ATP ratios among strains, crosses and backcrosses were performed as described in Sokal and Rohlf (1969, 1981).

Genetic distances between markers and *Gtpc* were determined using RI Manager (Manley & Elliot 1991) version 2.3. Briefly, the recombination fraction for a backcross population for any two loci is the ratio of recombinant animals to all informative animals. For RI strains, which arise from multiple generations of breeding, the probability of observing a recombinant is given by the relationship:

$$R = 4r/(1+6r)$$ (Haldane & Waddington 1931)

The quantity R is estimated from the proportion of recombinant strains in an RI set and r is estimated from R as follows:

$$r = R/(4-6R)$$

For backcrosses, the standard error of R:

$$s = R(1-R)/N$$

where N is the number of informative strains or animals.

For RI lines the standard error of r is:

$$s = (1+6r)\sqrt{[r(1+2r)/4N]}$$ Green (1981)

All graphs were produced using SigmaPlot® version 2.0. Strain distribution patterns obtained for microsatellite markers in the various recombinant inbred strains were compared to those in the Mouse Genome Database (Jackson Laboratories 1996).

Results

Survey of the Variability of Erythrocytic GTP and ATP Levels in Inbred Mouse Strains

To minimize triphosphate degradation, nucleotide extraction procedures need to be as efficient as possible. One way to monitor the amount of degradation is by assessing the ratio of ATP to ADP. The method used here for erythrocytic nucleotide extraction resulted in a mean erythrocytic ATP/ADP ratio of 9.5 ± 1.9. This is comparable to ratios reported previously in mouse (Jenuth *et al.* 1994), rat (Dean *et al.* 1978) and human erythrocytes (Dean *et al.* 1978; Simmonds *et al.* 1982, 1987, 1988).

No significant variation in erythrocytic ATP concentrations is evident amongst inbred mouse strains (Table 2, Figure 3). Assuming that all triphosphates degrade at an equal rate (see Jenuth *et al.* 1994), ATP measurements become a useful internal reference with regard to equivalence of extraction efficiency. Therefore, although the extraction method used appears to be effective in minimizing nucleoside triphosphate degradation, erythrocytic GTP concentrations were considered not only as absolute values but also as GTP/ATP ratios, in order to account for possible differences between samples.

Table 2. Erythrocytic purine nucleoside triphosphate concentrations (nmol/mL packed cells) in various inbred mouse strains.

Strain	GTP	ATP	GTP/ATP x 10^2
C3H/HeHa-*Pgk-1*^{a}	17 ± 2^a	731 ± 74	2.4 ± 0.3^i
NOD/Lt	23 ± 3^a	744 ± 24	3.1 ± 0.4^i
SWR/J	27 ± 15^a	844 ± 109	3.1 ± 1.3^i
BALB/cByJ	27 ± 3^a	723 ± 30	3.8 ± 0.6^i
I/LnJ	28 ± 3^a	1154 ± 251	2.5 ± 0.6^i
CD-1	29 ± 5^a	861 ± 126	3.5 ± 0.9^i
CDS/Lay	30 ± 9^a	831 ± 59	3.6 ± 0.8^i
SWV	30 ± 1^a	990 ± 115	3.1 ± 0.3^i
SIV	31 ± 4^a	959 ± 216	4.2 ± 0.9^i
SPRET-1	43 ± 13^a	911 ± 120	4.7 ± 1.1^i
WC/ReJ	46 ± 15^a	769 ± 149	5.8 ± 0.9^i
WB/ReJ	48 ± 6^a	915 ± 68	5.3 ± 0.4^i
B6-NPF	181 ± 13^b	894 ± 95	20.4 ± 1.7^{ii}
C57BL/6J-*c*/*c*	185 ± 25^{b,c}	773 ± 52	23.9 ± 2.5^{ii,iii}
CBA/FaCam	187 ± 26^{b,c}	678 ± 55	27.6 ± 4.1^{ii,iii,iv}
C57BL/6J	209 ± 34^{b,c}	771 ± 64	27.1 ± 2.2^{ii,iii,iv}
PERU W-1-II	220 ± 15^{b,c}	709 ± 46	31.2 ± 2.3^{iii,iv}
DBA/2J	229 ± 22^{b,c}	908 ± 76	25.3 ± 1.7^{ii,iii,iv}
In(X)1H	230 ± 69^{b,c}	1072 ± 376	22.6 ± 3.4^{ii}
SPLOTCH-RETARDED	276 ± 43^c	855 ± 166	32.7 ± 3.8^{iv}

Results are given as the mean ± standard deviation for n=5 animals. Comparisons amongst strains were carried out using Scheffé's analysis at p=0.01 (Sokal & Rohlf 1981). Results that do not differ significantly from one another are denoted by the same superscript, *a* through *c* for GTP concentrations, or *i* through *iv* for GTP/ATP ratios. No significant differences in ATP concentrations are evident amongst strains.

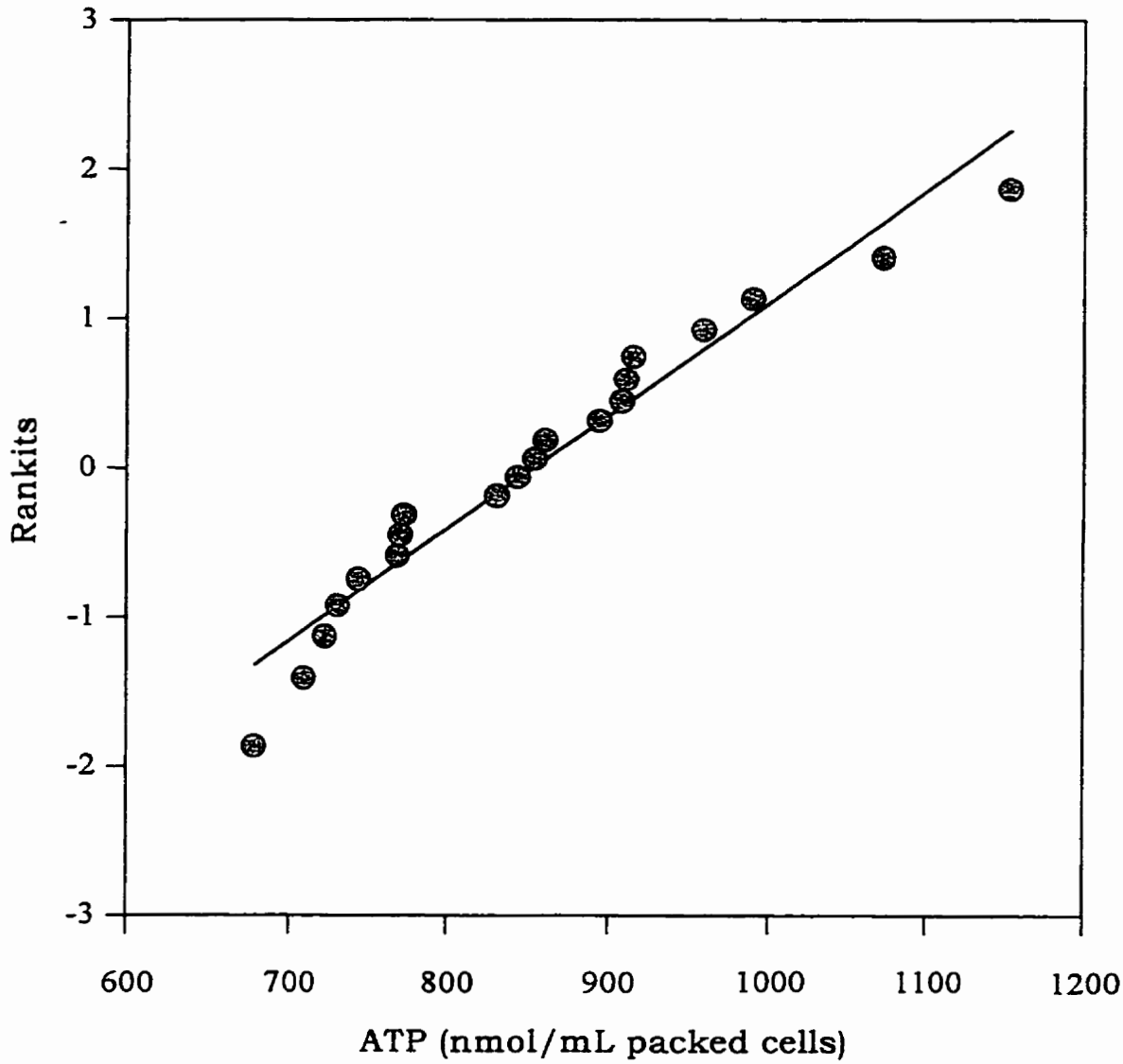

Figure 3. Rankit analysis (Sokal & Rohlf 1981) of erythrocytic ATP concentrations in various inbred mouse strains. Each circle represents the mean ATP concentration for an individual mouse strain. A first order regression line is shown.

Absolute GTP concentrations, given in ranked order in Table 2, show a 16-fold range in inbred mouse strains. When reported as a ratio of GTP/ATP, a 14-fold range is observed. Scheffé's analysis divides erythrocytic GTP concentrations into two distinct non-overlapping groups (Table 2). Mouse strains CBA/FaCam (CBA), B6-NPF, C57BL/6J-*c/c*, PERU W-1-II, C57BL/6J (B6), DBA/2J, In(X)1H, and SPLOTCH-RETARDED exhibit high GTP levels (181 - 276 nmol/mL erythrocytes), whereas C3H/HeHa-*Pgk-1*^{a}, NOD/Lt, CD-1, CDS/Lay, I/LnJ, SWV, SWR/J, BALB/cByJ, SIV, SPRET-1, WC/ReJ, and WB/ReJ (WB) exhibit low GTP levels (17 - 48 nmol/mL erythrocytes). The group with high GTP levels is split into two overlapping subgroups by Scheffé's tests, that is, a significant difference exists between the GTP concentrations of B6-NPF and SPLOTCH-RETARDED, but neither of these strains exhibits differences with respect to any other strain within the high GTP group.

Rankit analysis, which transforms ranked ordered deviates around a mean, segregates GTP levels into the same two distinct groups, indicated by first-order regression lines with differing slopes and intercepts (Figure 4). Results were also analyzed by Student-Newman-Keuls analysis (p=0.01) (not shown) and again shown to segregate into two distinct groups with respect to erythrocytic GTP concentrations. As with Scheffé's analysis, some heterogeneity within the group with high GTP levels was evident.

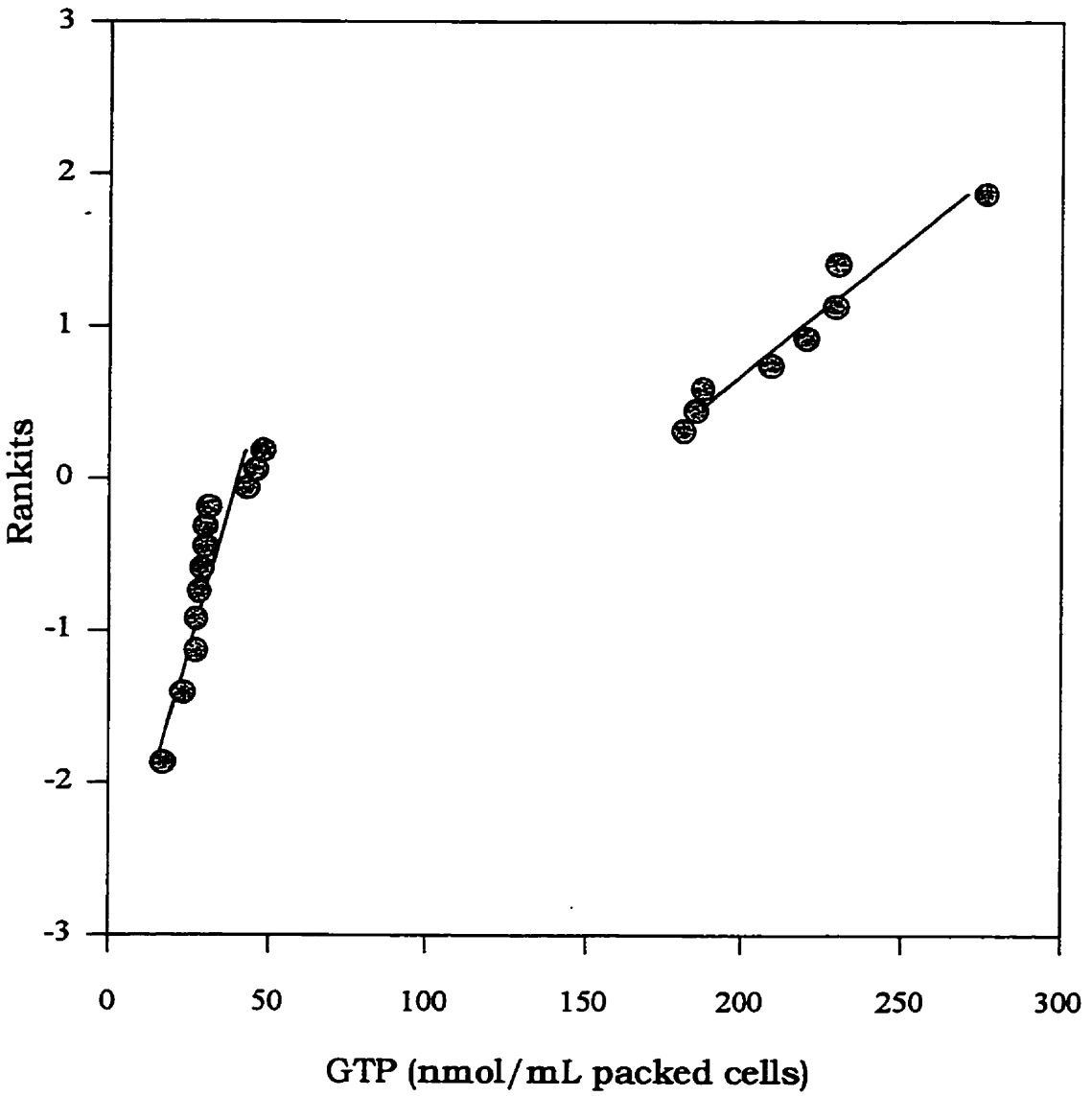

Figure 4. Rankit analysis (Sokal & Rohlf 1981) of erythrocytic GTP concentrations in various inbred mouse strains. Each circle represents the mean GTP concentration for an individual mouse strain. First order regression lines are shown.

The same two distinct groups are present in the analysis of GTP/ATP ratios (Table 2, Figure 5), with corresponding strains exhibiting either high GTP/ATP (x 10^2) ratios (20.4 - 32.7), or low ratios (2.4 - 5.3). Scheffé's analysis in this case finds four overlapping groups amongst the strains with higher GTP/ATP.

Erythrocytic nucleotide levels for the subspecies CAST-1 were not measured directly because this strain was unavailable, and are, therefore, not included in Table 2. Instead, (B6xCAST-1)F_1 and (CAST-1xB6)F_1 individuals were used. The direction of the cross did not alter the outcome (100 ± 0.3 nmol/mL packed cells and 99 ± 4 nmol/mL packed cells respectively, n=2). GTP levels for these F_1 mice are intermediate (99 ± 3 nmol/mL packed cells, n=4), that is, they fall between the two groups established in the strain survey. Since it is known that the B6 parent has high concentrations (209 ± 34 nmol/mL packed cells, n=5), it can be predicted that concentrations in CAST-1 red blood cells will fall within the low GTP category. This is based on previous observations that every examined (high GTP x low GTP strain) cross produced F_1's with intermediate GTP levels. GTP/ATP (x 10^2) ratios for these F_1 animals are comparably intermediate (12.9 ± 0.5) compared with B6 (27.1 ± 2.2), suggesting again that CAST-1 mice have low erythrocytic GTP levels.

Although no significant differences in ATP levels were found in this survey, a range of ATP concentrations was observed (723 – 1154

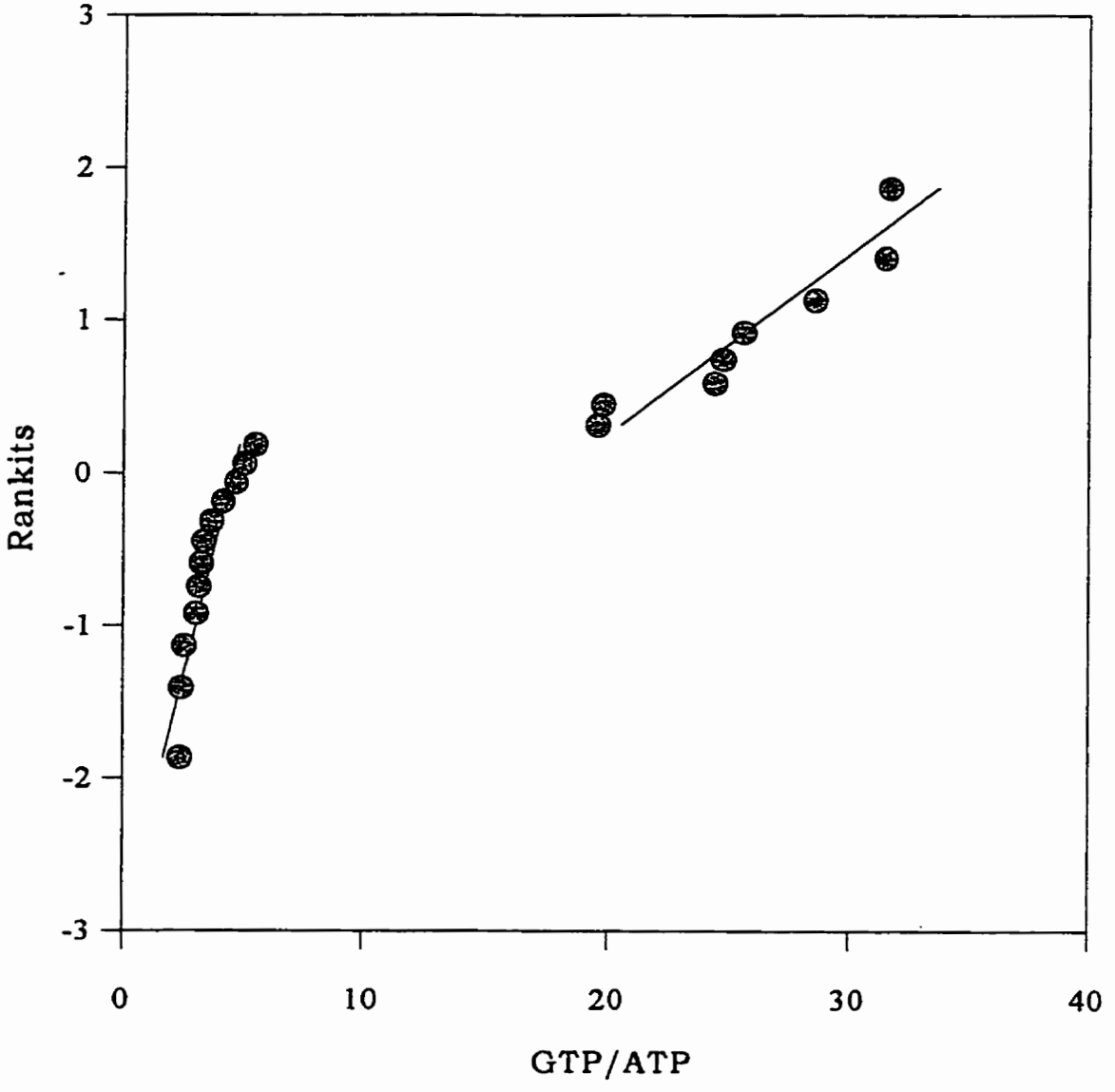

Figure 5. Rankit analysis (Sokal & Rohlf 1981) of erythrocytic GTP/ATP concentrations in various inbred mouse strains. Each circle represents the mean GTP/ATP for an individual strain. First order regression lines are shown.

nmol/mL packed cells). It was thought that perhaps there might be a correlation between adenosine and guanosine triphosphate levels, *i.e.* that all triphosphates might be elevated in one strain over another. That, however, was not observed. Nucleoside triphosphate levels appear to vary independently of one another. Strains with low GTP levels show a range of ATP levels (723 - 1154 nmol/mL packed cells), as do those with high GTP levels (678 - 1072 nmol/mL packed cells) (Figure 6).

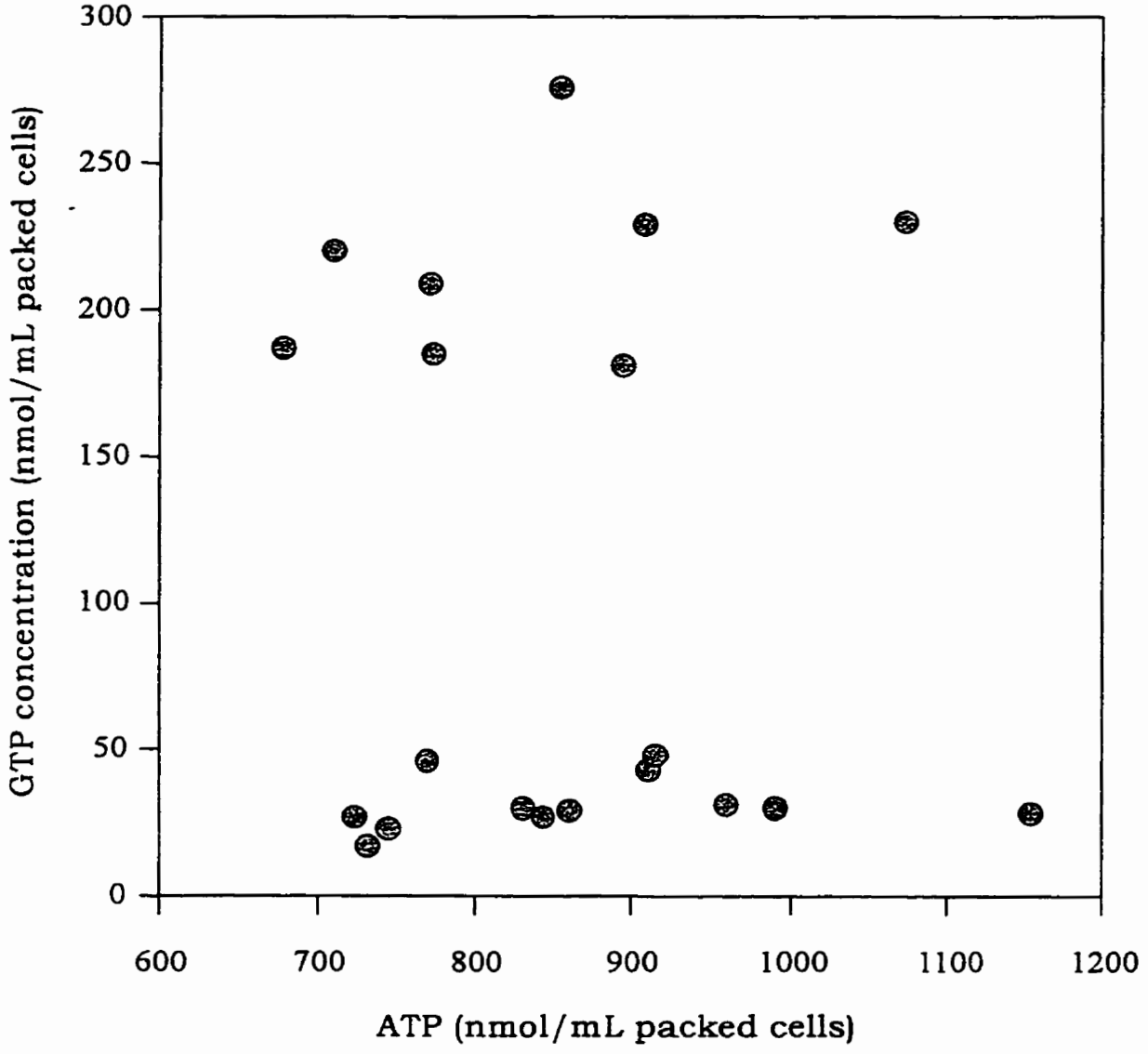

Figure 6. Erythrocytic GTP *versus* ATP concentrations of various inbred mouse strains. Each circle represents the mean GTP and ATP concentration for an individual mouse strain.

Assessment of the Variability of GTP/ATP Ratios in Nucleated Tissues

To ascertain whether cells other than erythrocytes also exhibit interstrain variations in GTP levels, nucleotides were extracted from C57BL/6J and C3H/HeHa-*Pgk-1*^{a} liver, kidney, brain, and tongue. These two strains were chosen to represent those exhibiting high and low erythrocytic GTP levels, respectively.

For all tissue nucleotide extractions the mean ATP/ADP ratio was 1.7 ± 0.4 (n=2 X 2 strains X 4 tissues =16). This value was considerably lower than that for erythrocytic nucleotide extractions, for which the ATP/ADP ratio was 9.5 ± 1.9 across all sampled strains (n=5 X 20 strains=100). The lower ATP/ADP ratios in tissues obtained here were comparable to those reported elsewhere (Childs *et al.* 1996; Jinnah *et al.* 1993). However, Guidotti *et al.* (1974) and Clark & Dar (1988) both reported that purine nucleotides undergo rapid degradation following the death of an animal. Due to methodological difficulties in sampling nucleotides in solid tissues *versus* erythrocytes, it is uncertain whether these values accurately reflect *in vivo* values, or indicate extensive triphosphate breakdown. Assuming that triphosphates degrade at an equivalent rate, and taking into account that ATP concentrations do not appear to vary between mouse strains, reporting GTP as a proportion of ATP (*i.e.* GTP/ATP ratios) should account for variations in extraction

efficiencies and normalize results between samples.

No interstrain differences in GTP concentrations were observed aside from that in erythrocytes (Table 3) (Scheffé's analysis p=0.01). However, the results of the tissue extractions do indicate the presence of tissue specific variation, with tongue having the lowest GTP/ATP ratio, and brain having the highest ratio.

Table 3. Tissue GTP/ATP (x 10^2) in C57BL/6J and C3H/HeHa·*Pgk-1*^{a} inbred mouse strains.

Cell/Tissue	C57BL/6J	C3H/HeHa·*Pgk-1*^{a}
liver	15.8 (14.6, 16.9)	15.1 (14.6, 15.5)
kidney	16.7 (16.1, 17.2)	16.3 (16.0, 16.5)
brain	23.4 (22.8, 24.0)	23.4 (21.8, 25.0)
tongue	4.2 (4.1, 4.3)	5.2 (5.0, 5.4)
erythrocyte (n=5)	27.1 ± 2.2	2.4 ± 0.3

Results are given as the mean followed by individual results in parentheses, or the mean ± standard deviation where n=5. C57BL/6J and C3H/HeHa·*Pgk-1*^{a} were chosen as the representative strains for high and low erythrocytic GTP/ATP ratios, respectively. No significant differences other than in erythrocytes were observed between strains (Scheffé's analysis p=0.01).

Mapping the Erythrocytic GTP Concentration Determining Trait (Gtpc) on Mouse Chromosome 9

The map position of *Gtpc* was refined using a [(B6XWB)F_1XB6] backcross. This backcross was used because B6 and WB strains have significantly different erythrocytic GTP levels (Table 2; Jenuth *et al.* 1994), and exhibit repeat length polymorphisms in the region of mouse chromosome 9 that is telomeric to *Trf*.

The genotype of *Gtpc* for each backcross individual was inferred by phenotypic assessment of erythrocytic GTP levels. In other words, homozygosity or heterozygosity at the *Gtpc* locus was based on whether each backcross offspring had high GTP levels (B6-like) or intermediate GTP levels (F_1-like), respectively. An example of nucleotides extracted from backcross individuals exhibiting high and intermediate GTP levels can be seen in Figure 7.

Since ATP levels did not differ significantly between the strains used to generate the backcrosses (Table 2), ATP levels were used as a control to normalize GTP levels, and results were reported as GTP/ATP ratios (Table 4). Of the 232 individuals typed, 124 B6-like and 108 F_1-like offspring were identified, in the expected 1:1 ratio (α=0.01).

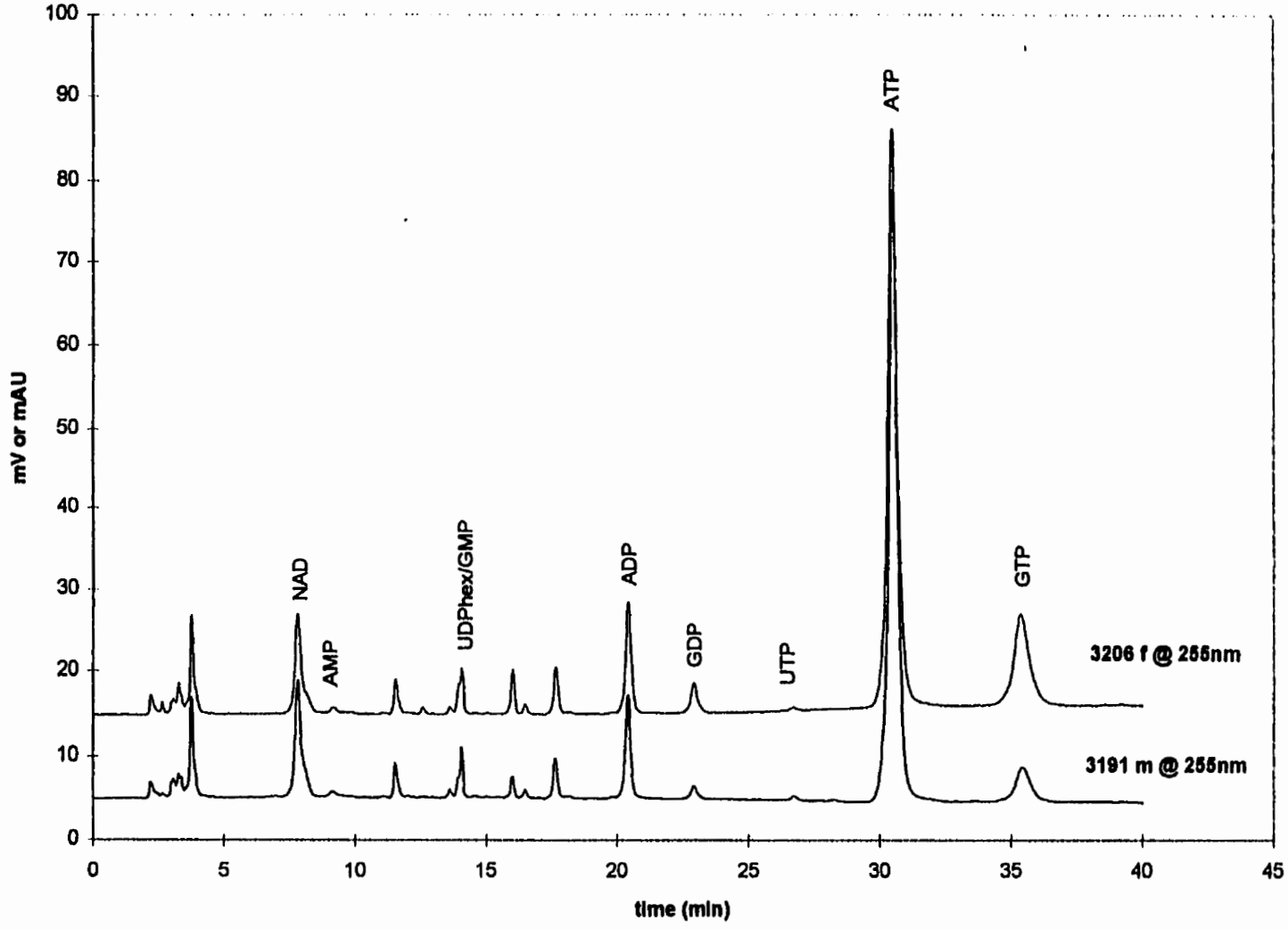

Figure 7. HPLC analysis of erythrocytic nucleotides extracted from two [(B6xWB)F_1xB6] backcross offspring. Note that 3206 f is B6-like with high levels of GTP, whereas 3191 m is F_1-like with intermediate levels of GTP.

Table 4. Representative erythrocytic GTP/ATP ratios of parental, F_1 and backcross mice used for mapping *Gtpc*.

Strain	GTP/ATP x 10^2
C57BL/6J (B6)	27.1 ± 2.2 [a]
WB/ReJ (WB)	5.3 ± 0.4 [b]
(B6xWB)F_1	16.7 ± 0.9 [c]
[(B6xWB)F_1xB6] backcross:	
- parental (B6)-like	27.2 ± 3.9 [a]
- F_1-like	13.9 ± 1.6 [c]

Results are given as the mean ± standard deviation for n=5 animals. GTP/ATP ratios that do not differ significantly from one another are indicated by the same letter, *a* through *c*, as determined by Scheffé's analysis (p=0.01) (Sokal & Rohlf 1981).

No differences in GTP/ATP ratios were noted between backcross offspring whose B6 parent was female rather than male (Table 5) (Scheffé's analysis p=0.01). In addition, sex-specific differences with respect to GTP/ATP ratios in backcross offspring were not observed (Table 6) (Scheffé's analysis p=0.01).

Table 5. Comparative erythrocytic GTP/ ATP levels in backcross offspring with a B6 female *versus* a B6 male parent.

	Backcross Parents	
	B6 female X F_1 male	F_1 female X B6 male
backcross offspring:		
high GTP/ATP x 10^2	26.8 ± 2.0 (n=15)^a	25.3 ± 3.5 (n=109)^a
low GTP/ATP x 10^2	12.8 ± 1.4 (n=9)^b	12.1 ± 1.8 (n=99)^b

Results are given as the mean ± standard deviation. GTP/ATP ratios that do not differ significantly from one another are indicated by the same letter, *a* or *b*, as determined by Scheffé's analysis (p=0.01) (Sokal & Rohlf 1981).

Table 6. Comparative erythrocytic GTP/ ATP levels in female *versus* male backcross offspring.

	[(B6xWB)F_1xB6] backcross	
	females	males
high GTP/ATP x 10^2	26.3 ± 3.1 (n=64)^a	24.6 ± 3.5 (n=60)^a
low GTP/ATP x 10^2	12.8 ± 1.7 (n=58)^b	11.4 ± 1.6 (n=50)^b

Results are given as the mean ± standard deviation. GTP/ATP ratios that do not differ significantly from one another are indicated by the same letter, *a* or *b*, as determined by Scheffé's analysis (p=0.01) (Sokal & Rohlf 1981).

Eight microsatellite markers, which were informative for B6 and WB, and located near *Gtpc*, were applied to typing the backcross progeny. The sizes of microsatellite amplification products used to map *Gtpc* are given in Table 7, and examples of amplification products are shown in Figure 8. The following gene order and genetic distances were generated (in cM ± S.E.): (*D9Mit14*) 0.4±0.4 (*D9Mit24*) 1.7±0.8 (*Gtpc, D9Mit51, D9Mit116, D9Mit212*) 3.9±1.3 (*D9Mit200*) 3.0±1.1(*D9Mit20*) 7.8±1.8 (*D9Mit18*) (Figures 9 & 10).

In any backcross, it is the F_1 individual from which recombination events, contributing to the genetic distance, are being scored. It is generally thought that genetic distance is substantially larger in females than in males (Dietrich *et al.* 1994). The total genetic distance reported here for pooled crosses is 16.8 ± 2.5 cM. The direction of the cross does not appear to make a difference for this part of mouse chromosome 9; backcrosses in which the F_1 is female generate a distance of 16.8 ± 2.6 cM, compared to that of 16.7 ± 7.6 cM in which the F_1 is male.

Table 7. Amplification product lengths of microsatellite markers used to map *Gtpc* in [(B6xWB)F_1xB6] backcross mice.

Microsatellite Marker	**C57BL/6J* (B6)**	**WB/ReJ** (WB)**
D9Mit14	78 bp	60 bp
D9Mit18	180 bp	214 bp
D9Mit20	110 bp	105 bp
D9Mit24	125 bp	135 bp
D9Mit51	124 bp	140 bp
D9Mit116	132 bp	140 bp
D9Mit200	147 bp	133 bp
D9Mit212	108 bp	120 bp

* C57BL/6J product lengths are taken from the Murine MapPairs™ Research Genetics April 1995 release.

** WB/ReJ product lengths were estimated relative to DNA molecular weight marker V (Boehringer Mannheim) as a standard.

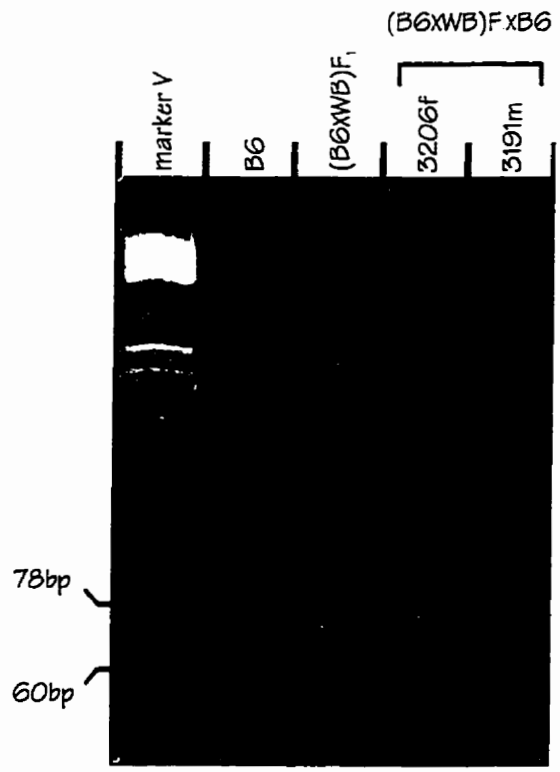

Figure 8. Amplification products of microsatellite marker *D9Mit14* from B6, (B6xWB)F_1, and [(B6xWB)F_1xB6] mice. Note that 3206f is parental-like, whereas 3191m is F_1-like and shows both 78bp and 60bp amplification products.

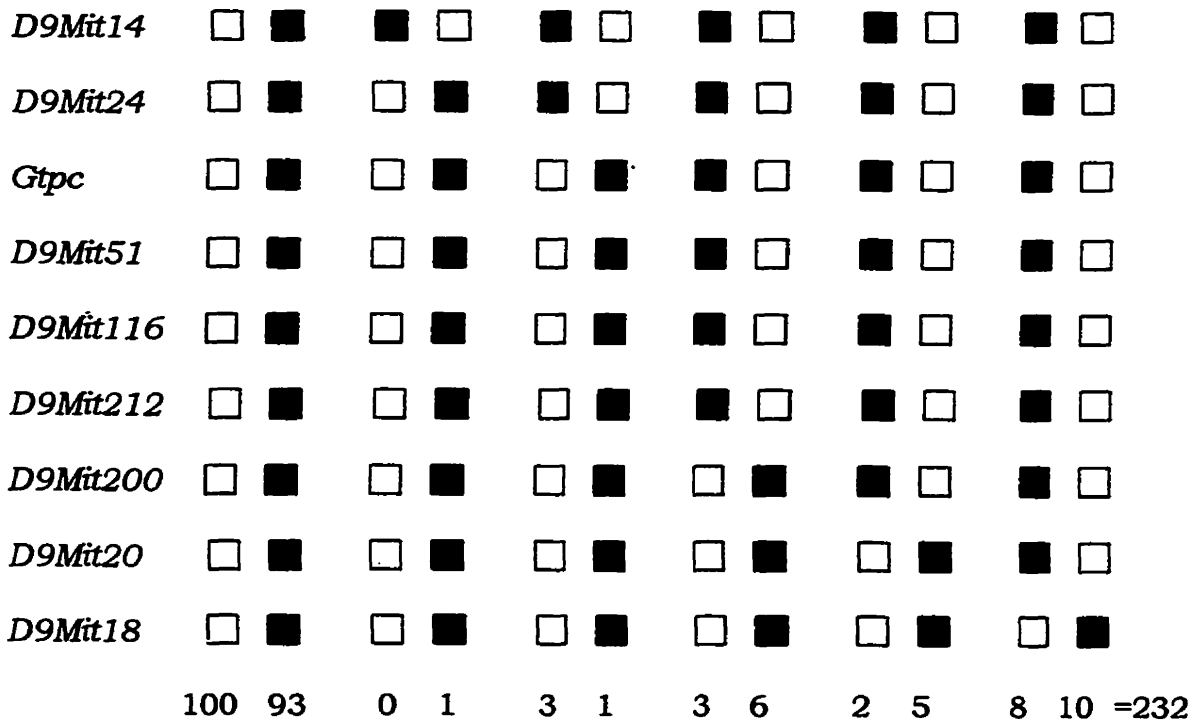

Figure 9. Numbers of [(B6XWB)F_1XB6] backcross progeny exhibiting the given genotype at each locus; either as measured by polymorphic microsatellite markers, or, for *Gtpc*, as is inferred by the phenotypic assessment of erythrocytic GTP levels. Open boxes represent mice homozygous for the B6 allele. Shaded boxes represent mice heterozygous for both the WB and the B6 alleles. Paired columns represent reciprocal genotypes.

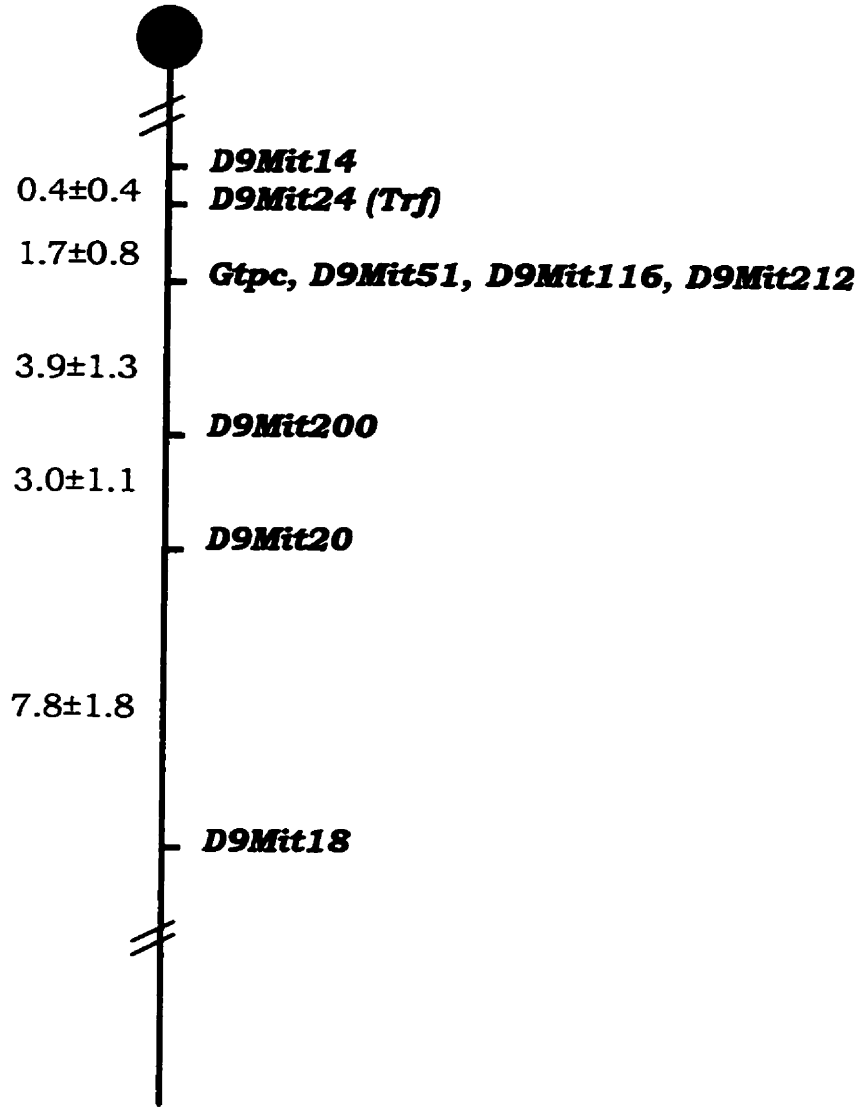

Figure 10. Regional genetic map of mouse chromosome 9. Genetic distances are given in cM ± S.E.

Mapping the Gtpc-Informative Microsatellite Markers in Recombinant Inbred Strains

Genomic DNA from BXH, BXA, AXB, and BXD RI lines was typed for the same microsatellite markers that were used to localize *Gtpc* in the [(B6XWB)F_1XB6] backcross. The typing was performed to refine the region surrounding *Gtpc* on mouse chromosome 9, and to establish the order amongst those markers showing no recombination with *Gtpc* (*i.e. D9Mit51, D9Mit116, D9Mit212*) (Figures 9 & 10).

Initially, microsatellites were amplified from RI progenitor strains to look for the presence of distinguishable length polymorphisms (Table 8). Polymorphic markers were subsequently amplified from the corresponding RI strains. An example of typing the BXH RI strain set is shown in Figure 11. The strain distribution patterns that were generated for the four RI sets are given in Tables 9-12. All coding loci and their corresponding strain distribution patterns shown in Tables 9-12 were taken from the Mouse Genome Database (July 1996). They have been included as points of reference to link the strain distribution patterns generated here to those existing in the literature. The distances between markers were then determined and used to generate the genetic maps of this sub-region of chromosome 9 in the RI strains (Figure 12.)

Table 8. Amplification product lengths of microsatellite markers used to map *Gtpc* in AXB, BXA, BXD and BXH recombinant inbred strains.

Microsatellite	Parental Strains			
Marker	**A/J (A)**	**C57BL/6J (B)**	**DBA/2J (D)**	**C3H/HeJ (H)**
D9Mit14	60 bp	78 bp	78 bp*	60 bp
D9Mit18	210 bp	180 bp	180 bp*	210 bp
D9Mit20	113 bp	110 bp	103 bp	113 bp*
D9Mit24	133 bp	125 bp	125 bp*	133 bp
D9Mit51	134 bp	124 bp	134 bp	134 bp
D9Mit116	142 bp	132 bp	140 bp	142 bp
D9Mit200	143 bp	147 bp	133 bp	143 bp
D9Mit212	120 bp	108 bp	118 bp	120 bp

Letters in brackets following the strain name refer to the abbreviated form used in the recombinant inbred strain nomenclature. The amplification product lengths for *D9Mit18* in DBA/2J and for *D9Mit14* in strains other than C57BL/6J were estimated relative to DNA molecular weight marker V (Boehringer Mannheim) as a standard. All other product lengths are taken from the Murine MapPairs™ Research Genetics April 1995 release.

* These products could not be differentiated from the corresponding C57BL/6J products using 4% agarose gel electrophoresis; *D9Mit14*, *D9Mit18* and *D9Mit24* were not typed in the BXD RI strains, and *D9Mit20* was not typed in the BXH RI strains.

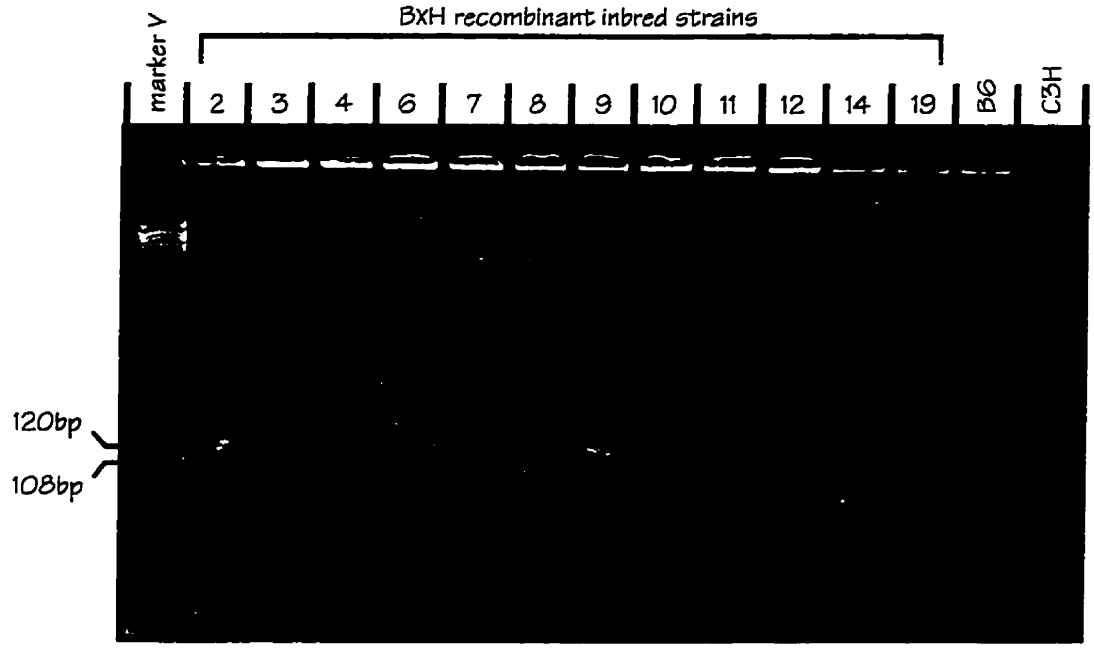

Figure 11. Amplification products of microsatellite marker *D9Mit212* from BXH recombinant inbred strains.

Table 9. BXH strain distribution patterns of microsatellite markers used to map *Gtpc*.

Locus	BXH Recombinant Inbred Strains 2	3	4	6	7	8	9	10	11	12	14	19	References
D9Mit14	**H**	**H**	**B**	**B**	**B**	**H**	**H**	**B**	**B**	**H**	**B**	**H**	
D9Mit24	**H**	**H**	**B**	**B**	**B**	**H**	**H**	**B**	**B**	**H**	**B**	**H**	
D9Mit51	**H**	**H**	**B**	**B**	**B**	**H**	**H**	**B**	**B**	**H**	**B**	**H**	
D9Mit200	**H**	**H**	**B**	**B**	**B**	**H**	**H**	**B**	**B**	**H**	**B**	**H**	
				x									
Gtpc	H	H	B	H	B	H	H	B	B	H	B	H	Jenuth *et al.* 1994
D9Mit116	**H**	**H**	**B**	**H**	**B**	**H**	**H**	**B**	**B**	**H**	**B**	**H**	
D9Mit212	**H**	**H**	**B**	**H**	**B**	**H**	**H**	**B**	**B**	**H**	**B**	**H**	
Kfo1	H	H	B	H	B	H	H	B	B	H	B	H	Elliott 1979
Ltw3	H	H	B	H	B	H	H	B	B	H	B	H	Elliott 1979
Fv2	H	H	B	H	B	H	H	B	B	H	B	H	Jenkins *et al.* 1982
								x					
Rbp2	H	H	B	H	B	H	H	H	B	H	B	H	Nass *et al.* 1993
Pitr6	H	H	B	H	*	H	H	H	B	H	B	H	Frankel & Coffin 1994
D9Mit16	H	H	B	H	B	H	H	H	B	H	B	H	Vagliani *et al.* 1993
Bgl	H	H	B	H	B	H	H	H	B	H	B	H	Lalley *et al.* 1982
									x				
D9Mit18	**H**	**H**	**B**	**H**	**B**	**H**	**H**	**H**	**H**	**H**	**B**	**H**	Vagliani *et al.* 1993; Taylor & Reifsnyder 1993
			x										
Ctt1	H	H	H	H	B	H	H	H	H	H	B	H	Vagliani *et al.* 1993

• not given

Strain distribution patterns (SDPs) for markers in bold are work of this thesis. SDPs for previously typed loci within this region of mouse chromosome 9 are also included and have been ordered to produce the least number of crossovers. Note that the SDP for marker *D9Mit18*, although confirmed as part of this study, was previously established.

Table 10. AXB strain distribution patterns of microsatellite markers used to map *Gtpc*.

Locus	AXB Recombinant Inbred Strains																						References
	1	2	3	4	5	6	7	8	9	10	11	12	13	14	15	17	18	19	20	21	23	24	
D9Mit14	**A**	**A**	**B**	**A**	**B**	**B**	**B**	**B**	**B**	**B**	**A**	**B**	**A**	**A**	**B**	**B**	**A**	**A**	**A**	**A**	**A**	**B**	
D9Mit24	**A**	**A**	**B**	**A**	**B**	**B**	**B**	**B**	**B**	**B**	**A**	**B**	**A**	**A**	**B**	**B**	**A**	**A**	**A**	**A**	**A**	**B**	
											x				**x**								
D9Mit51	**A**	**A**	**B**	**A**	**B**	**B**	**B**	**B**	**B**	**B**	**B**	**B**	**A**	**A**	**A**	**B**	**A**	**A**	**A**	**A**	**A**	**B**	
												x											
Gnai2	A	A	*	A	B	B	B	B	B	B	B	A	A	A	A	B	A	A	A	A	A	B	Blatt *et al.* 1988
												?											
Gnat1	A	A	B	A	B	B	B	B	B	B	B	*	A	A	A	B	A	A	A	A	A	B	Blatt *et al.* 1988
							x					**?**											
D9Mit116	**A**	**A**	**B**	**A**	**B**	**B**	**A**	**B**	**B**	**B**	**B**	**B**	**A**	**A**	**A**	**B**	**A**	**A**	**A**	**A**	**A**	**B**	
D9Mit212	**A**	**A**	**B**	**A**	**B**	**B**	**A**	**B**	**B**	**B**	**B**	**B**	**A**	**A**	**A**	**B**	**A**	**A**	**A**	**A**	**A**	**B**	
						x						**x**											
D9Mit200	**A**	**A**	**B**	**A**	**B**	**A**	**A**	**B**	**B**	**B**	**B**	**A**	**A**	**A**	**A**	**B**	**A**	**A**	**A**	**A**	**A**	**B**	
D9Mit20	**A**	**A**	**B**	**A**	**B**	**A**	**A**	**B**	**B**	**B**	**B**	**A**	**A**	**A**	**A**	**B**	**A**	**A**	**A**	**A**	**A**	**B**	
										x													
D9Mit16	A	A	B	A	B	A	A	B	B	A	B	A	A	A	A	B	A	A	A	A	A	B	Naggert *et al.* 1997
				x																**x**			
Bgl	A	A	B	B	B	A	A	B	B	*	B	A	*	A	*	*	*	A	*	B	A	*	Youngblood *et al.* 1989
							x													**x**			
D9J1	A	A	B	B	B	A	B	B	B	A	B	A	A	A	A	B	A	A	A	A	A	B	Cheah *et al.* 1994
D9Mit18	**A**	**A**	**B**	**B**	**B**	**A**	**B**	**B**	**B**	**A**	**B**	**A**	**A**	**A**	**A**	**B**	**A**	**A**	**A**	**A**	**A**	**B**	**Mu *et al.* 1992**

*** - not given ? - the exact position of the crossover is not known due to ambiguities in one of the SDPs.**
Strain distribution patterns (SDPs) for markers in bold are work of this thesis. SDPs for previously typed loci within this region of mouse chromosome 9 are also included and have been ordered to produce the least number of crossovers. Note that the SDP for marker *D9Mit18*, although confirmed as part of this study, was previously established.

Table 11. BXA strain distribution patterns of microsatellite markers used to map *Gtpc*.

Locus	BXA Recombinant Inbred Strains																		References
	1	2	4	7	8	9	11	12	13	14	16	17	18	20	22	23	24	25	26	
D9Mit14	**B**	**A**	**A**	**A**	**B**	**A**	**B**	**A**	**A**	**B**	**A**	**B**	**A**	**B**	**A**	**B**	**B**	**A**	**B**	
D9Mit24	**B**	**A**	**A**	**A**	**B**	**A**	**B**	**A**	**A**	**B**	**A**	**B**	**A**	**B**	**A**	**B**	**B**	**A**	**B**	
			x																	
D9Mit51	**B**	**A**	**B**	**A**	**B**	**A**	**B**	**A**	**A**	**B**	**A**	**B**	**A**	**B**	**A**	**B**	**B**	**A**	**B**	
D9Mit116	**B**	**A**	**B**	**A**	**B**	**A**	**B**	**A**	**A**	**B**	**A**	**B**	**A**	**B**	**A**	**B**	**B**	**A**	**B**	
D9Mit212	**B**	**A**	**B**	**A**	**B**	**A**	**B**	**A**	**A**	**B**	**A**	**B**	**A**	**B**	**A**	**B**	**B**	**A**	**B**	
Gnai2	B	A	B	A	B	A	B	A	A	B	A	B	A	B	A	B	B	A	*	Blatt *et al.* 1988
	?																			
Gnat1	*	A	B	A	B	A	B	A	A	B	A	B	A	B	A	B	B	A	*	Blatt *et al.* 1988
	?														**x**			**x**		
D9Mit200	**A**	**A**	**B**	**A**	**B**	**A**	**B**	**A**	**A**	**B**	**A**	**B**	**A**	**B**	**B**	**B**	**B**	**B**	**B**	
D9Mit20	**A**	**A**	**B**	**A**	**B**	**A**	**B**	**A**	**A**	**B**	**A**	**B**	**A**	**B**	**B**	**B**	**B**	**B**	**B**	
								x	**x**											
D9Mit16	A	A	B	A	B	A	B	B	B	B	A	B	A	B	B	B	B	B	B	Naggert *et al.* 1997
								x									**x**			
Bgl	A	*	B	A	*	A	B	A	B	*	*	B	*	*	B	B	A	*	*	Youngblood *et al.* 1989
						x		**x**												
D9J1	A	A	B	A	B	B	B	B	B	B	A	B	A	B	B	B	A	B	B	Cheah *et al.* 1994
D9Mit18	**A**	**A**	**B**	**A**	**B**	**B**	**B**	**B**	**B**	**B**	**A**	**B**	**A**	**B**	**B**	**B**	**A**	**B**	**B**	**Mu *et al.* 1992**

*** - not given ? - the exact position of the crossover is not known due to ambiguities in one of the SDPs.**
Strain distribution patterns (SDPs) for markers in bold are work of this thesis. SDPs for previously typed loci within this region of mouse chromosome 9 are also included and have been ordered to produce the least number of crossovers. Note that the SDP for marker *D9Mit18*, although confirmed as part of this study, was previously established.

Table 12. BXD strain distribution patterns of microsatellite markers used to map *Gtpc*.

	BXD Recombinant Inbred Strains																									
Locus	**1**	**2**	**5**	**6**	**8**	**9**	**11**	**12**	**13**	**14**	**15**	**16**	**18**	**19**	**20**	**21**	**22**	**23**	**24**	**25**	**27**	**28**	**29**	**30**	**31**	**32**
D9Byu3	D	B	B	D	D	B	B	D	B	B	B	D	D	B	D	D	D	B	B	D	B	B	B	D	B	D
Rbp2	D	B	B	D	D	B	B	D	B	B	B	B	D	*	D	D	D	B	B	D	B	B	B	D	B	B
D9byu4	D	B	B	D	D	B	B	B	B	B	B	B	D	B	D	B	D	B	B	D	B	D	B	B	B	D
Ltw3	D	B	B	D	D	B	B	B	B	B	B	B	*	B	D	B	D	B	B	D	B	B	B	B	B	*
D9Mit51	**D**	**B**	**B**	**D**	**D**	**B**	**B**	**B**	**B**	**B**	**B**	**B**	**D**	**B**	**D**	**B**	**D**	**B**	**B**	**D**	**B**	**B**	**B**	**B**	**B**	**D**
Gnat1	D	B	B	B	D	B	B	B	B	B	B	B	D	D	D	B	D	B	B	D	B	B	B	B	D	D
Fv2	D	B	B	B	D	B	B	B	B	B	B	B	D	B	D	B	D	D	B	D	D	B	B	B	*	*
D9Mit116	**D**	**D**	**B**	**B**	**D**	**B**	**B**	**B**	**B**	**B**	**B**	**B**	**D**	**B**	**D**	**B**	**D**	**D**	**B**	**D**	**D**	**B**	**B**	**B**	**D**	**D**
D9Mit212	**D**	**D**	**B**	**B**	**D**	**B**	**B**	**B**	**B**	**B**	**B**	**B**	**D**	**B**	**D**	**B**	**D**	**D**	**B**	**D**	**D**	**B**	**B**	**B**	**D**	**D**
D9Mit15	*	D	B	B	D	B	B	B	B	B	B	B	D	B	D	B	D	D	B	D	B	B	B	*	*	*
Pltr6	D	D	B	B	D	B	B	B	B	B	B	D	B	D	D	D	*	D	B	D	B	B	B	B	D	D
D9Mit200	**D**	**D**	**B**	**B**	**D**	**B**	**B**	**B**	**B**	**B**	**B**	**B**	**D**	**B**	**D**	**D**	**D**	**D**	**B**	**D**	**B**	**B**	**B**	**B**	**D**	**D**
D9Mit20	**B**	**D**	**B**	**B**	**D**	**B**	**B**	**B**	**B**	**B**	**B**	**B**	**D**	**B**	**D**	**D**	**D**	**B**	**B**	**D**	**B**	**B**	**B**	**B**	**D**	**D**
Bgl	B	D	B	B	D	B	B	B	B	B	B	B	D	B	D	D	D	B	B	D	B	B	B	B	D	*
Bgl-s	*	D	*	B	D	B	B	*	B	B	*	B	D	B	D	D	D	*	B	D	B	B	B	B	*	*
D9Mit18	*	D	B	D	B	B	B	B	B	B	B	D	B	B	B	D	D	D	B	B	B	B	B	*	*	*
D9Byu5	D	D	B	D	B	B	B	B	B	B	B	D	B	B	B	D	D	D	D	B	B	B	B	D	B	D
Cck	B	D	B	D	B	B	B	B	B	B	B	D	B	B	B	D	D	D	D	B	B	B	B	D	B	D
D9Byu6	B	D	B	D	B	B	B	B	B	D	B	D	B	B	B	D	D	D	D	B	B	B	B	D	B	D

* - not given ? - the exact position of the crossover is not known due to ambiguities in one of the SDPs.
Strain distribution patterns (SDPs) for markers in bold are work of this thesis. SDPs for previously typed loci within this region of mouse chromosome 9 are also included and have been ordered to produce the least number of crossovers. Note that the SDP for marker *D9Mit20*, although confirmed as part of this study, was also previously established (Table 13).

Table 13. References corresponding to BXD strain distribution patterns reported in Table 12.

Locus	References
D9Byu3	Woodward *et al.* 1992
Rbp2	Nass *et al.* 1993; Demmer *et al.* 1987
D9byu4	Woodward *et al.* 1992
Ltw3	Nadeau *et al.* 1981; Elliot *et al.* 1978
Gnat1	Blatt *et al.* 1988
Fv2	Elliot *et al.* 1978
D9Mit15	Dietrich *et al.* 1992
Pltr6	Frankel & Coffin 1994
D9Mit20	Dietrich *et al.* 1992
Bgl	Breen *et al.* 1977
Bgl-s	Meisler 1976
D9Mit18	Dietrich *et al.* 1992
D9Byu5	Woodward *et al.* 1992
Cck	Elliot & Yen 1991; Friedman *et al.* 1989
D9Byu6	Woodward *et al.* 1992

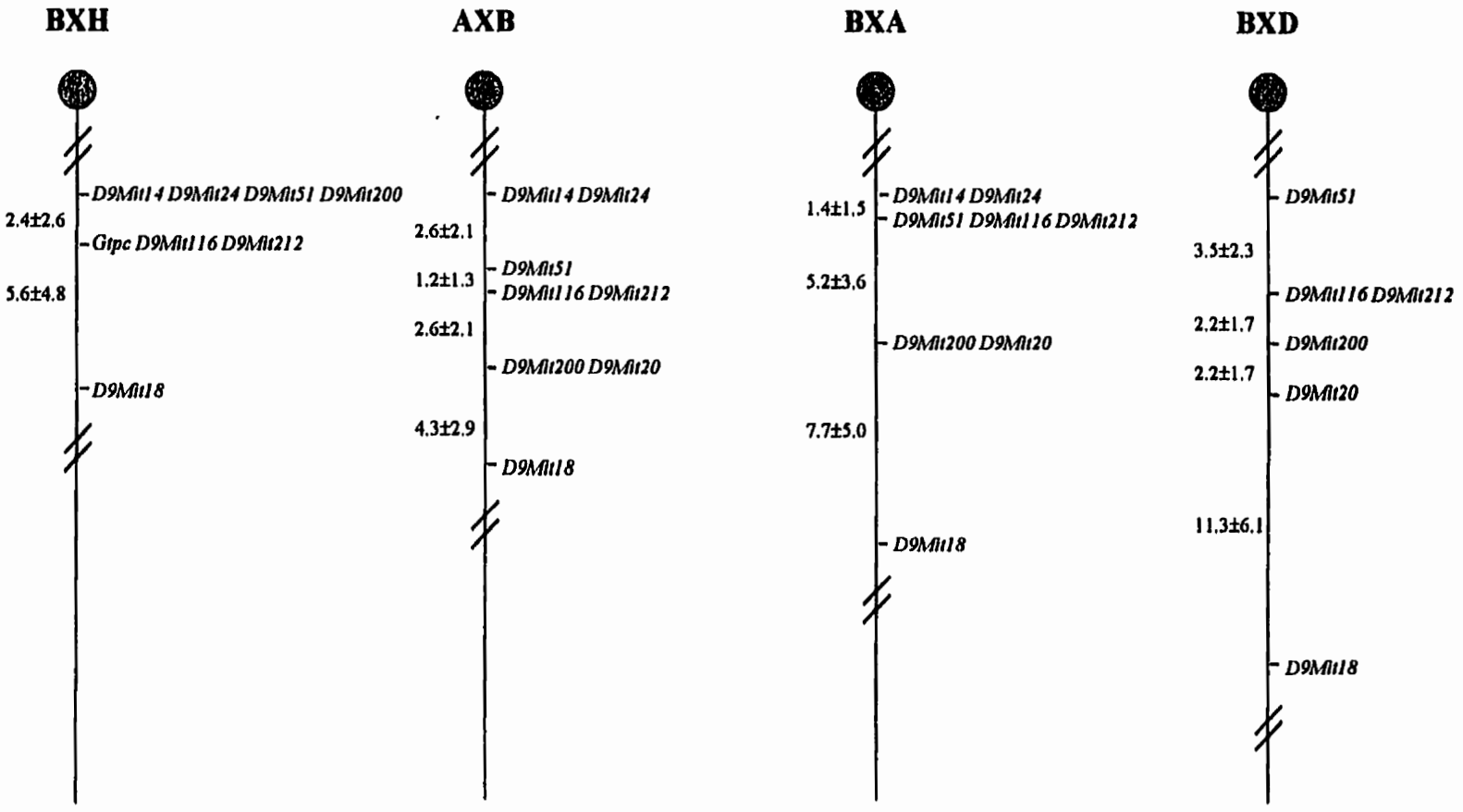

Figure 12. Regional genetic map of mouse chromosome 9 for recombinant inbred strains BXH, AXB, BXA and BXD. Genetic distances are given in cM ± S.E.

Assessment of Candidate Gene Products of Gtpc

The metabolism of substrates IMP, GMP and GTP was studied in B6 and WB mice to determine whether differences existed between these two strains which could account for the observed differences in erythrocytic GTP concentrations (Table 2). First, the rate of production of XMP and GMP from IMP was measured by HPLC. Secondly, to assess the rate of GTP catabolism, the production of GDP, GMP, guanosine, guanine and xanthine was followed. Finally, the rate of GMP degradation was observed by measuring the accumulation of guanosine, guanine and xanthine (refer to the purine pathway in Figure 1).

No differences in the metabolism of GTP or IMP were detected between erythrocytic lysates from B6 and WB mice (data not shown). There was, however, a marked difference in the catabolism of GMP. WB lysates had a 2-fold increase in the breakdown of GMP, and a resulting 2-fold increase in the production of xanthine compared with B6 lysates after 60 minutes (Figure 13 & 14). Since this was the only part of the purine metabolic pathway to show any interstrain differences, GMP catabolism became the target for further study.

The rate of GMP breakdown was measured using a coupled assay in which the final product could be measured spectrophotometrically (Figure 2). The idea behind this assay is that a certain step of the

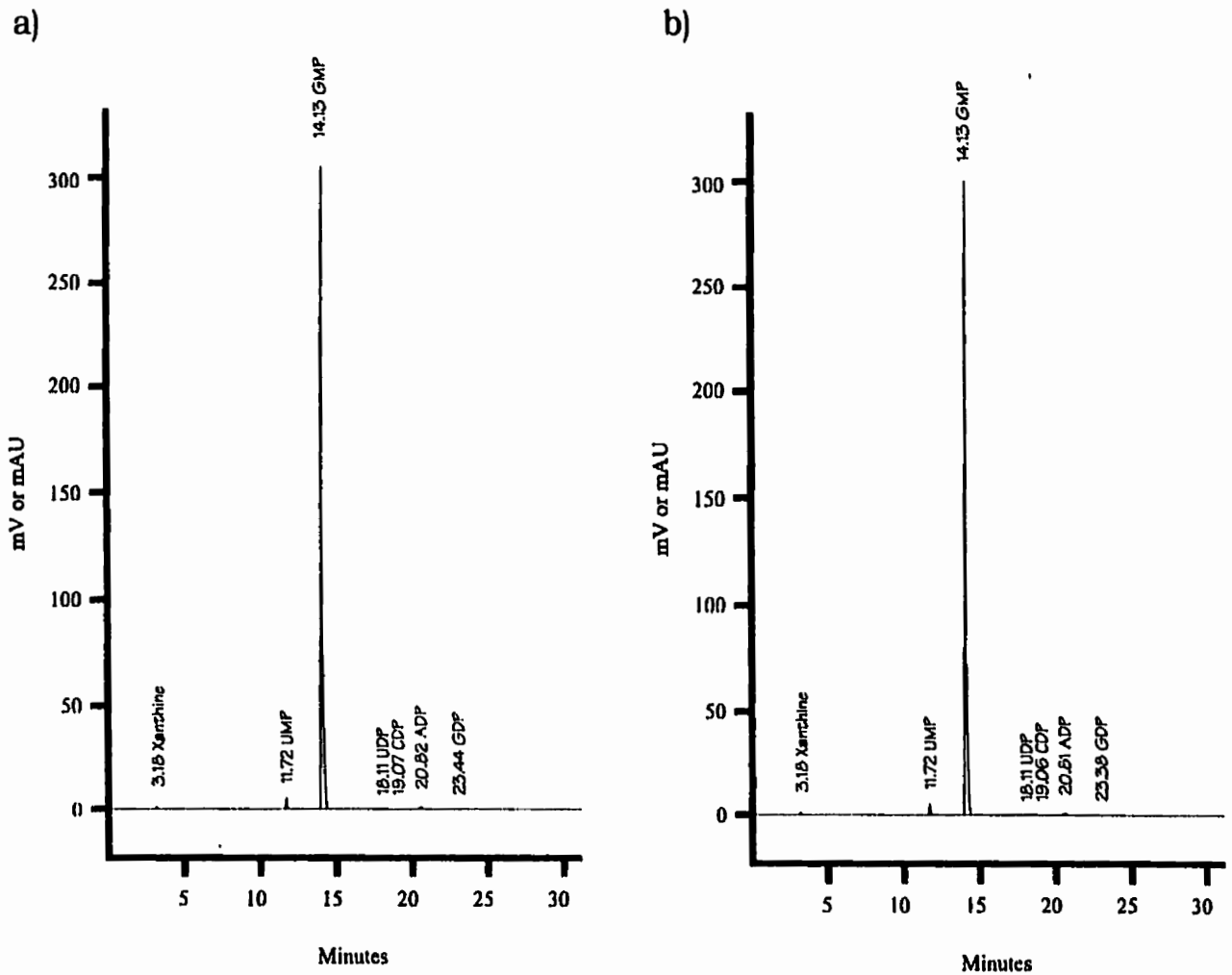

Figure 13. HPLC analysis of erythrocytic nucleotides extracted from a) B6 and b) WB lysates incubated with GMP for 0 minutes. Note the equivalent xanthine and GMP peaks.

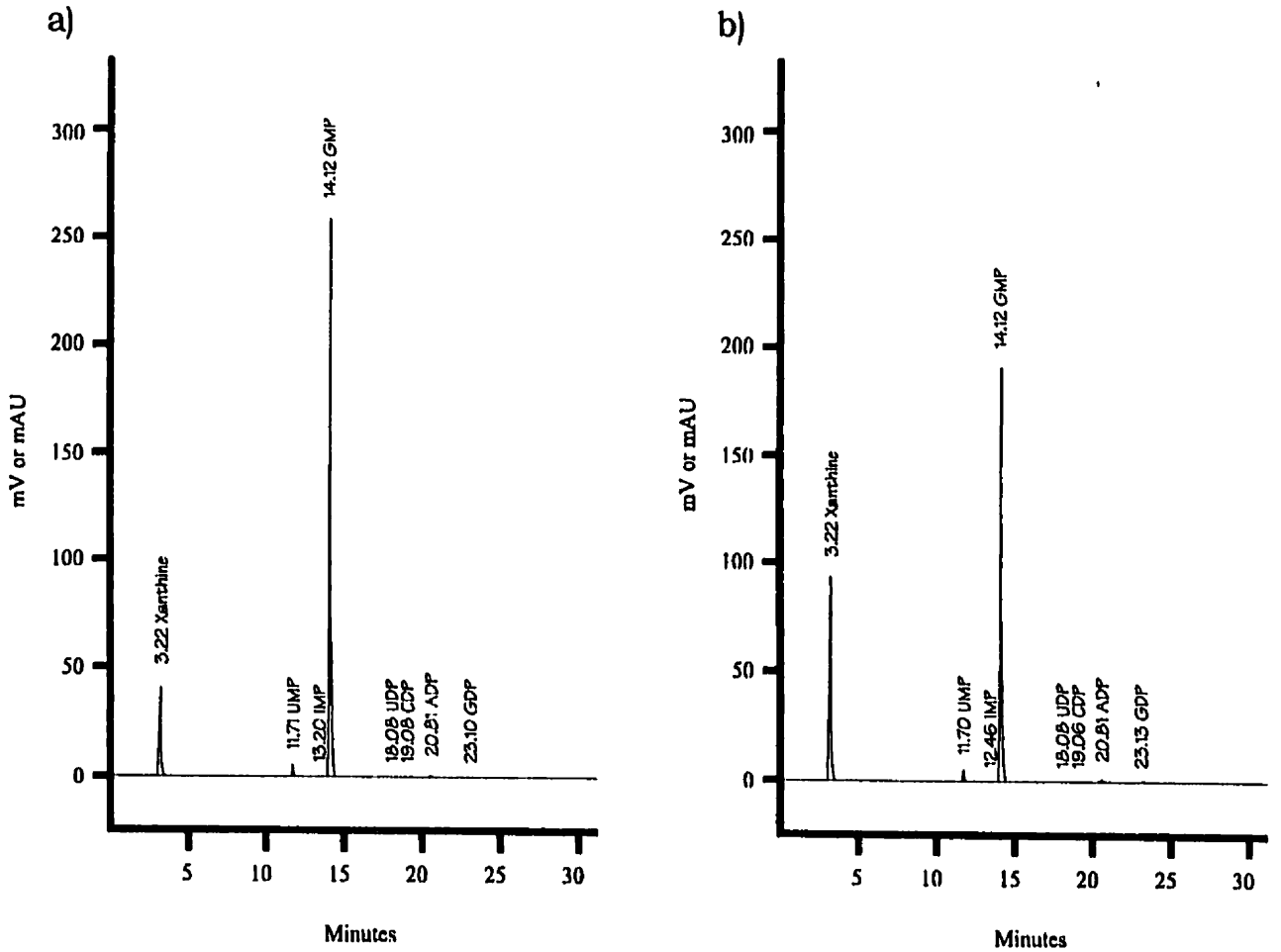

Figure 14. HPLC analysis of erythrocytic nucleotides extracted from a) B6 and b) WB lysates incubated with GMP for 60 minutes. Note that there is a 2-fold reduction in GMP and a corresponding 2-fold increase in xanthine in WB *versus* B6.

pathway can be monitored if the steps after the one of interest proceed in a non-rate-limiting manner, *i.e.* the step of interest should be the rate-limiting one. Then, because it is rate-limiting, the rate at which the reaction proceeds is equal to the rate at which the step of interest proceeds. In this case, the rate of conversion of GMP to guanosine was of interest (Figure 2). Therefore, the further catabolism of guanosine should proceed uninhibited in order to measure the rate of the enzymatic reaction that produces guanosine. The best way to ensure that this portion of the pathway is not rate-limiting is to add the appropriate enzymes so that they are present in excess. However, guanine deaminase and purine nucleoside phosphorylase were not added to the reaction mixture, to determine whether endogenous amounts of these two enzymes would be sufficient.

A number of guanosine concentrations were used to determine at what point the rate of reaction no longer increased. Maximal velocity was realized at 0.5 mM. This guanosine concentration was then used as a substrate for both B6 and WB erythrocytic lysates. The rate of product formation did not vary significantly between strains. The same range finding was performed for GMP as a substrate, and it was determined that the rate of reaction no longer increased at 2 mM. The rate of reaction using guanosine as a substrate was greater than that with GMP as a substrate, indicating that the rate-limiting step was the conversion

of GMP to guanosine. This confirmed that the endogenous amounts of purine nucleoside phosphorylase and guanine deaminase were enough to be non-rate-limiting.

The above conditions were then applied to pooled erythrocytic lysates from B6 and WB mice. The outcome was a 20% increase in the rate of GMP catabolism in WB lysates (0.650 nmol/(minute · mg protein)) as compared to B6 (0.542 nmol/(minute · mg protein)). These preliminary results suggest a difference in reaction rates for the 5'-nucleotidase catalyzing the GMP to guanosine conversion in inbred strains with varying *Gtpc* phenotypes.

Discussion

Erythrocytic GTP and ATP Levels in Inbred Mouse Strains

The data presented herein clearly indicates that strain-specific erythrocytic GTP levels can be divided into two distinct groups: those strains exhibiting high GTP concentrations (215 ± 44 nmol/mL packed cells) and those exhibiting low GTP concentrations (34 ± 12 nmol/mL packed cells) (Table 2). The division between the upper and lower strains suggests there are at least two allelic forms of *Gtpc*, the gene that governs erythrocytic GTP levels in the mouse. Scheffé's test indicates some heterogeneity within the group with high GTP levels. This may point to the existence of more *Gtpc* alleles, or may suggest the influence of the strain background; *i.e.* other loci may be implicated which have a lesser effect on erythrocytic GTP concentrations. This is not unexpected when one considers the participation of GTP in a number of biochemical events. Variability in the rate of GTP utilization by any of a large number of biological processes could affect the overall concentration of GTP within the cell. Variability could also arise from alterations to any of the enzymes directly involved in its synthesis.

Mouse strains other than common laboratory inbred strains, SPRET-1 (*Mus spretus*) and PERU W1-II (*Mus musculus domesticus*), were

included in this survey to search for further variation in GTP levels. Since these strains are more distantly related, it was expected that the number of phenotypic variants of erythrocytic GTP concentration would increase. This, however, was not the case (Table 2). PERU W1-II, which has high erythrocytic GTP levels (220 ± 15 nmol/mL packed cells), does not differ significantly from the seven laboratory strains also having high GTP levels. Similarly, SPRET-1, with low GTP levels (43 ± 13 nmol/mL packed cells), shows no significant differences with the 11 laboratory strains also in this low GTP level grouping.

Lack of GTP Variability in Nucleated Tissues

Erythrocytes are terminally differentiated cells, devoid of nuclei, mitochondria or ribosomes. As such, no *de novo* protein production occurs within these cells. It was therefore important to determine whether the varying levels of GTP observed in mouse red blood cells were simply due to an altered half-life of a GTP regulating enzyme, or if some other mechanism involving the rate of GTP synthesis or degradation was at work.

No interstrain differences in GTP levels in cells other than erythrocytes were observed (Table 3). These observations also hold true

for heart (Wiebe, Fung & Snyder, unpublished results) and spleen leukocytes (Jenuth, Fung & Snyder, unpublished results). This suggests that GTP levels may be indicative of enzymatic polymorphisms leading to different activity levels or altered half-lives which manifest only within the differentiated state of the erythrocyte. The argument would be that in cells other than erythrocytes, the continued production of proteins would be able to maintain GTP at the necessary levels. However, in the erythrocyte, the machinery required to make such proteins is lost during the final stage of differentiation. Cell functions can then only be carried out by the proteins already present. For instance, if a protein such as GMP 5'-nucleotidase had significantly different half-life between strains, guanine nucleotides would not be broken down to the same extent, leading to relatively higher GTP levels. This would also be true if the same enzyme had a lower activity level.

Since erythrocytes have a finite life span (47-57 days in the mouse (Landaw & Winchell 1970)), it is presumed that what is actually being measured is the average level of GTP across the erythrocyte populations. It would be of interest to look at samples of red-blood cells of the same age to see how GTP concentrations change over the life span of the erythrocyte, and how they vary between strains. Landaw and Winchell (1970) reported significant variations in erythrocytic life-span between three different mouse strains. With respect to GTP levels, it could

therefore be argued that what is being measured might not actually be directly related to GTP production or breakdown, but may be a side affect of having a younger average erythrocyte population.

It would also be interesting to look at reticulocytes (immature erythrocytes) which are also anucleate, but still maintain ribosomes and therefore the capability of translation (if not transcription), to see whether their GTP concentrations also vary across mouse strains. Russell *et al.* (1951) looked at reticulocytes in 18 different inbred mouse strains, and found that reticulocytes varied from 1.5% - 3.5% of total blood cells amongst strains. Unfortunately, no statistical analyses were performed to determine if these values were significantly different.

The lack of GTP variability observed in other tissues makes the pursuit of the *Gtpc* gene product no less important. Paglia and Valentine (1980) discovered a pyrimidine-specific nucleotidase through the study of hereditary nonspherocytic hemolytic anemia, which results in significantly increased erythrocytic CTP, TTP, and UTP levels. Therefore, the study of GTP levels in mouse red blood cells may point to another as yet unidentified component of GTP catabolism.

Variability of GTP Levels Between Tissues

Within a single mouse strain, variations in GTP/ATP ratios between tissues were noted (Table 3). Tongue had the lowest ratio, which was not unexpected. Since tongue is primarily muscle, it would have a higher ATP requirement than the other tissues sampled. Muscle contraction is driven by the interaction between actin and myosin, which is coupled to the hydrolysis of ATP.

Brain had the highest GTP/ATP ratio, which may be due to the higher requirement of GTP for use in neurotransmitter production. GTP is required to produce the co-factor tetrahydrobiopterin, which in turn is essential for dopamine, norepinephrine, epinephrine, serotonin, and melatonin synthesis. For example, the inability to utilize GTP to produce tetrahydrobiopterin is known to be related to a form of hereditary progressive dystonia (Ichinose *et al.* 1994).

Genetic Mapping of the Erythrocytic GTP Concentration Determining Trait (Gtpc) on Mouse Chromosome 9

Genetic mapping has been greatly facilitated by the identification of microsatellite markers, which occur at high frequency throughout the

mouse genome and tend to exhibit length polymorphism. Microsatellites, or simple sequence repeats (SSRs), may be readily assayed by the polymerase chain reaction (PCR) using unique flanking regions (Love *et al.* 1990; Dietrich *et al.* 1992, 1994). Over 6000 simple sequence length polymorphisms (SSLPs) have been identified to date between mouse strains C57BL/6J-ob/ob (OB) and CAST/Ei (CAST). Strains OB and CAST were used because they represent different subspecies; CAST is *Mus musculus castaneus*, whereas laboratory strains (OB) arise from *Mus musculus domesticus* and *Mus musculus musculus* progenitors. As such, these strains are expected to be somewhat distant genetically, resulting in a higher number of polymorphisms, while still producing fertile F_1 offspring, making them more useful in genetic studies.

Using SSLPs, a genetic map has been constructed which provides an average spacing of 0.25 cM between markers, corresponding to approximately 500 kb of DNA. Of the identified SSRs, approximately 50% are expected to be polymorphic between laboratory strains arising from the same progenitor lines, compared to the 94% rate of polymorphism observed between species or subspecies. Nonetheless, the informative microsatellite markers available between laboratory strains facilitate the fine mapping of most genes.

Over two hundred backcross individuals have been typed for GTP levels and eight microsatellite markers to localize *Gtpc* to a 5.6 ± 2.1 cM

region flanked by markers *D9Mit24* and *D9Mit200* (Figures 9 & 10). No recombination events were observed between *Gtpc* and three microsatellite markers, *D9Mit51*, *D9Mit116*, and *D9Mit212*. Marker *D9Mit24* was identified within *Trf* through a search of Genbank for simple tandem repeats by Dietrich *et al.* (1992). This marker was specifically used here as a reference to link these results to the existing map, as *Trf* has been designated as one of eight reference markers on chromosome 9 (Kingsley 1993). Since the position of *Trf* has already been defined, the map of mouse chromosome 9 generated in this study is linked to genetic position 56 and cytogenetic position F1-3 (Kingsley 1993; Baranov *et al.* 1987).

The microsatellite marker map presented here differs from recently published maps compiled by the MIT Center for Genome Research (July 1997) and the Mouse Genome Database (MGD) (July 1997) (Figure 15). The total genetic distance generated for this region of mouse chromosome 9 using the [B6xWB)F_1xB6] backcross is 16.8 ± 2.5 cM compared to that reported by MIT (12.1 cM) and MGD (15 cM).

Markers *D9Mit116*, *D9Mit212*, *D9Mit200*, and *D9Mit20* have not previously shown any recombination. No recombinants between markers *D9Mit116* and *D9Mit212* were observed in this study, but this pair was determined to be located proximal to *D9Mit200*, which in turn lies proximal to *D9Mit20* (Figures 9 & 10). Conversely, *D9Mit51*, reported by MIT to be 1.1 cM proximal to *D9Mit116* and *D9Mit212*, did not recombine in this study

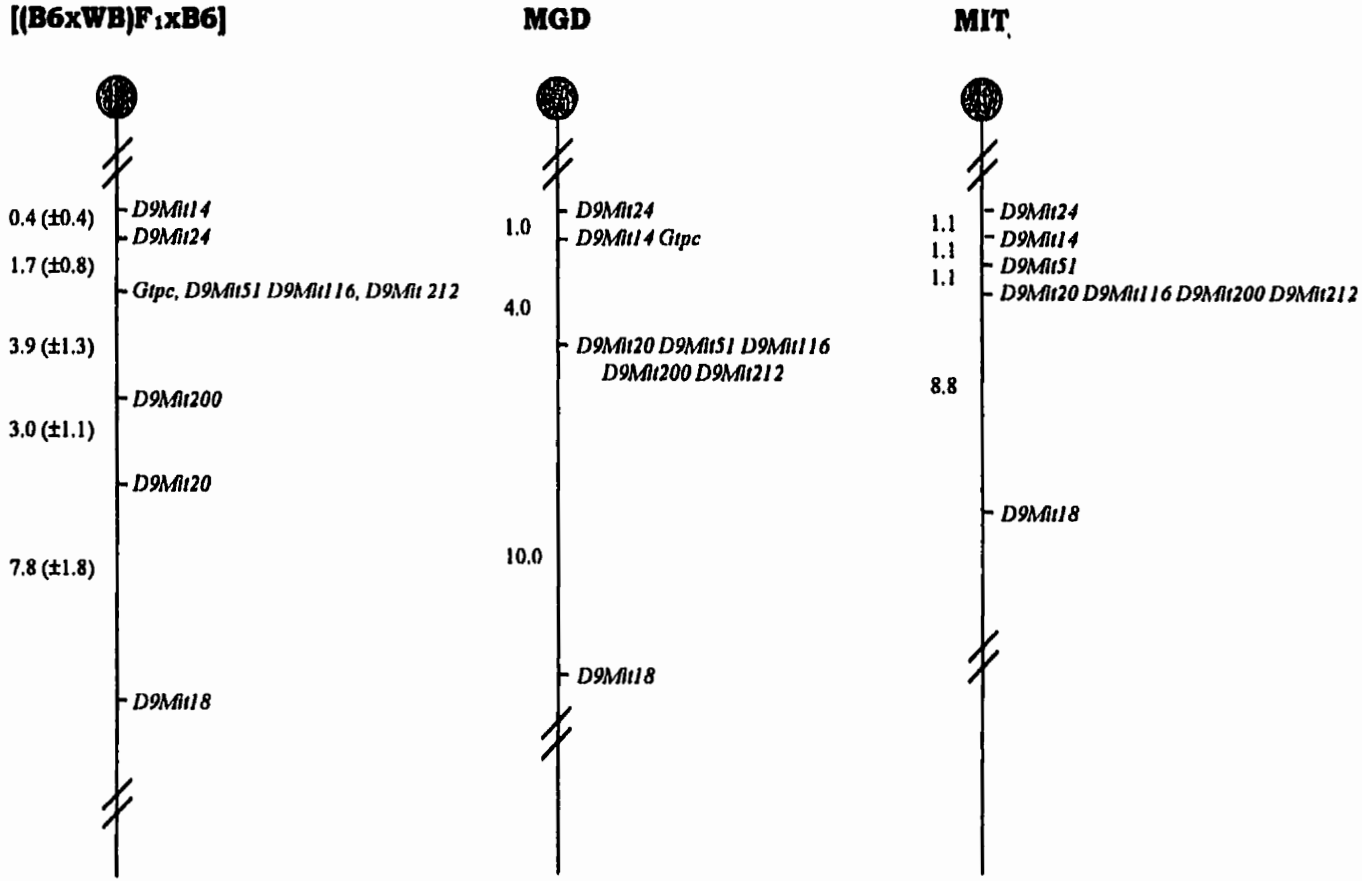

Figure 15. A comparison of the regional genetic map of mouse chromosome 9 generated by this study (using [(B6xWB)F_1xB6] backcross analysis), the Mouse Genome Database (July 1997), and the MIT Center for Genome Research (July 1997). Genetic distances are given in cM (± S.E.). Marker *D9Mit24* is located within *Trf* and therefore anchors the above maps at genetic position 56 and cytogenetic position F1-3 (Dietrich *et al.* 1992; Kingsley 1993; Baranov *et al.* 1989)

with either of those markers in the backcrosses typed. At a distance of 1.1 cM, out of 232 individuals, two to three crossover events between those markers would be expected. It should be noted that MIT markers are mapped based on 92 informative meioses, and therefore only one recombination event was observed between *D9Mit51* and the other two markers. A chance recombination event in a smaller number of informative meioses could artificially inflate the actual distance between these markers.

One other difference between the map generated here and those reported elsewhere is that, based on a single recombination event, this work places the position of *D9Mit14* proximal, rather than distal, to *Trf*. If what was observed in this study was actually a double crossover event, the reported map order would be maintained. However, due to the proximity of these two markers to one another, it is unlikely that a double crossover has occurred.

Variations in genetic maps may occur as a result of different sample sizes. Like *D9Mit51*, many of the microsatellite markers have been previously mapped using 46 intercross offspring (Dietrich *et al.* 1992), corresponding to 92 informative meioses, compared to the 232 informative meioses from the (B6XWB)F_1XB6 backcross offspring typed here. Variations may also be indicative of biological differences in recombination frequencies between strains used (Dietrich *et al.* 1992). The (OBXCAST) intercross uses the subspecies *Mus musculus castaneus* (CAST), which was chosen to

maximize the observed microsatellite polymorphisms. However, polymorphism between CAST and laboratory inbred strains may not be limited to lengths of simple sequence repeats. Because these strains are more distantly related, differences may also extend to gene order, distances between repeats or distributions of recombinational events (Copeland *et al.* 1993). Dietrich et al. (1994) reported a recombination "hot-spot" near the telomere of chromosome 19 in (CASTxB6)F_2 crosses, which was not observed by Eicher and Shown (1993) using a [(SPRETxB6)xB6] backcross. A cross based solely on laboratory inbred strains might therefore be expected to give slightly different results.

Gtpc-Informative Microsatellite Markers in Recombinant Inbred Strains

Recombinant inbred (RI) strains arise through the systematic inbreeding of two pre-existing progenitor strains (Bailey 1971). Descendants of randomly mated pairs of F_2 individuals are continuously brother-sister mated for twenty or more generations. More than 98 percent of the polymorphic loci in the resulting RI strains are expected to be genetically fixed. Alleles of unlinked loci are randomized in the F_2 generation, and are expected to be fixed in parental and recombinant allelic combinations with equal probability. Linked genes, on the other

hand, have a tendency to remain together in parental allelic combinations.

Each RI strain is equally likely to have inherited either the maternal or paternal progenitor strain allele at each autosomal locus. Therefore, a trait such as *Gtpc*, which is under the control of a single gene that differ in the progenitors, is expected to resemble one of the progenitor strains approximately one-half of the time. The parental strains used to generate each of the sets are designated in the name using the following abbreviations A - A/J, B - C57BL/6J, D - DBA/2J, H - C3H/HeJ. For example, the AXB recombinant inbred strain set arises from A/J and C57BL/6J parents.

Strain distribution patterns (SDPs) were generated in BXH, AXB, BXA, and BXD recombinant inbred (RI) strains, for each of the markers showing polymorphisms between the respective progenitor strains (Tables 8-12). With one exception, the order of the markers did not change, although the distances varied between the different RI strains. The only difference of note occurred in the BXH strains. Marker *D9Mit200* generated the same SDP as markers *D9Mit14*, *D9Mit24*, and *D9Mit51*. Ordering the markers according to fewest number of recombination events between SDPs would then place *D9Mit200* proximal, rather than distal to *Gtpc*, *D9Mit116* and *D9Mit212*, as found in the backcross analysis, and in all other RI strains. This may indicate a

difference in order in the BXH strains, or it may be that two crossovers have occurred between *D9Mit200* and those markers with which it shares SDPs.

It should also be noted that *D9Mit51* segregated from *D9Mit116* and *D9Mit212* in BXH, AXB and BXD recombinant inbred strains, but did not segregate in the [(B6XWB)F_1XB6] backcross.

Gtpc Candidate Gene Products

To continue to refine the *Gtpc* locus, more microsatellite markers could be used to narrow the distance between flanking markers. A smaller total genetic distance would greatly facilitate the switch to physical mapping. Yeast artificial chromosome (YAC) libraries are available, which are pooled and sub-pooled in such a way that a minimal number of polymerase chain reactions could be employed to find the appropriate clone with the sequence of interest. However, the markers known to flank *Gtpc* at this point are roughly 5 cM apart, corresponding to about 10,000 kb. Assuming that the average size of a YAC insert is 500 kb, a minimum of 20 YACs would need to be screened. This would necessitate making a contiguous map of this region. Work is being carried out by the European Collaborative Interspecific Backcross

project, and the MIT Center for Genome Research to create a physical map. This will be integrated with the genetic map, but it will be some time before such a tool is available for use in localizing mouse genes. An alternate approach to searching the physical map for likely coding regions or previously mapped genes is to assess candidate gene products for identity with *Gtpc*.

Candidate genes to be considered for identity with *Gtpc* include those genes whose products are known to affect the rate of GTP anabolism or catabolism. There are a number of genes or gene products, listed in Table 14, which could possibly be responsible for the observed differences in erythrocytic GTP levels. Altered activities of any one of these could potentially affect GTP concentrations. Products of genes known to map to locations other than the region of interest on chromosome 9 have been excluded. For example, hypoxanthine-guanine phosphoribosyl transferase has been previously mapped to the X-chromosome (Chapman *et al.* 1983). Purine nucleoside phosphorylase and GTP cyclohydrolase have both been mapped to mouse chromosomes 14 (Womack *et al.* 1977; Ichinose *et al.* 1995).

The region of mouse chromosome 9 that is distal to *Trf* exhibits synteny only to human chromosome 3p21-23 (MGD July 1997). Therefore, although many of the candidates in Table 14 have not yet been mapped in the mouse, they may be eliminated based on the syntenic

Table 14. Potential gene products responsible for erythrocytic GTP variations.

Gene Product	Chromosomal Location
GTP synthesis:	
IMP dehydrogenase I	unknown
IMP dehydrogenase II	unknown
GMP synthase	unknown
GMP kinase	unknown
GTP degradation/utilization:	
GMP nucleotidase	unknown
GMP reductase	unknown
guanine deaminase	unknown
G proteins - Gnat1	9
- Gnai2	9
tubulin	unknown
elongation factors - EF1	unknown
- EF2	unknown
initiation factor - eIF2	unknown
release factor - RF1	unknown
guanylate cylase	unknown
adenylosuccinate synthase	unknown

relationship of their position in the human genome. This would limit the list of potential candidates to IMPDH II, GNAT1 and GNAI2, which have all been mapped to 3p in humans (Glesne *et al.* 1993; Blatt *et al.* 1988), and to GMP synthase, GMP nucleotidase, guanine deaminase, eIF2 and RF-1, which have not yet been mapped.

The genes encoding two G-proteins, *Gnat1*, and *Gnai2*, have been mapped in the mouse to the same region on chromosome 9 where *Gtpc* is located (Blatt *et al.* 1988; Drivas *et al.* 1990, 1991). Conserved regions of the proteins are thought to bind and hydrolyze guanine nucleotides, whereas divergent regions may play a role in subcellular localization and protein interaction. G-proteins participate in the process of signal transduction through interaction with effector molecules, which in turn generate second messenger molecules. Some G-proteins play a role in actin polymerization as part of maintaining cellular structure. It is conceivable that alterations to G-proteins may affect the rate of usage of GTP and therefore intercellular concentrations of GTP pools.

Gnat1 and *Gnai2* were mapped using RFLP analysis of mouse genomic DNA using probes derived from bovine retina, and rat epithelium, respectively. Tissue distribution studies have found the bovine GNAT1 transcripts to be found only in retinal rod photoreceptors (Lerea *et al.* 1986), and so it seems unlikely that GNAT2 would be responsible for controlling erythrocytic GTP levels. Rat GNAI2

transcripts, on the other hand, have been found in many tissues including brain, heart, kidney, lung, intestine and olfactory cells (Jones & Reed 1987), making GNAI2 a much more likely candidate. Although G-proteins possess intrinsic GTPase activity, the question remains as to whether the small amount of GTP these proteins actually hydrolyze would be enough to result in the observed differences in erythrocytic GTP levels.

IMP dehydrogenase has not yet been mapped in the mouse, but its map position on human chromosome 3 (3p21.2-p24.2) is syntenic to the region of interest (Glesne *et al.* 1993; Kingsley 1993; Nadeau *et al.* 1992). This enzyme is a good candidate for *Gtpc* because, in addition to its syntenic map position, it is known to catalyze the rate-limiting step in the *de novo* biosynthetic pathway of GTP (Snyder & Henderson 1973). Experiments involving rat hepatoma 3924A cells showed that during the biochemical proliferative stage, there was a redirection in the utilization of the radiolabel from IMP (Natsumeda *et al.* 1988). The result was an 8-fold rise in the ratio of guanylate to adenylate synthesis. When tiazofurin, a potent inhibitor of IMPDH, is present, a decrease in guanylate metabolism is observed, and there is a noticeable oncolytic response in hepatoma-carrying rats (Lui *et al.* 1984).

Other studies were performed on a mouse neuroblastoma cell line that exhibited a 10,000-fold increased resistance to mycophenolic acid,

an inhibitor of IMPDH (Hodges *et al.* 1989). A 2-fold increase in GTP levels was observed compared with wild-type neuroblastoma cells. Upon removal of mycophenolic acid, there was a further 2-fold increase in GTP concentrations. A 25-fold increase in IMPDH gene copy number was found in the resistant cells, however, mRNA levels had increased 500-fold (Lightfoot & Snyder 1994). Although gene amplification had occurred, it was not enough to explain the much higher mRNA levels. Since IMPDH gene expression has been determined to be inversely regulated by intracellular guanine ribonucleotide concentrations (Glesne *et al.* 1991), it may follow that a decrease in the effectiveness of end product regulation has occurred.

Based on these studies, the different erythrocytic GTP levels exhibited in laboratory mouse strains could be explained by an alteration in IMPDH. This may either be due to an increased amount of IMPDH (from increased gene expression prior to terminal differentiation), or due to a change in its enzymatic activity.

A metabolic investigational approach was undertaken to discover the identity of the putative *Gtpc* gene product. The number of candidates could be restricted by determining whether the differences in GTP pools occur as a result of alterations in its synthesis or degradation.
To look at enzymes involved in *de novo* GTP synthesis (IMPDH, GMP synthase, and GMP kinase), IMP was added to follow the formation of

XMP, GMP, GDP and GTP. In order to study catabolism, GTP or GMP was added, and the rate of degradation products was monitored, to provide information on GMP nucleotidase, GMP reductase, guanine deaminase, and GTPases. Both types of assays employed in this study used erythrocyte samples pooled from several individuals.

Preliminary results suggest that an enzyme involved in GMP catabolism, possibly a GMP-specific 5'-nucleotidase may be responsible for the differences seen in GTP levels. Further analysis would require optimization of conditions for an assay specifically designed to look at this step of catabolism. GMP 5'-nucleotidase requires the presence of a bivalent metal salts (e.g. Mg^{2+}) (Itoh 1981) and ATP for complete activity (Van den Berghe *et al.* 1977). The second (colourimetric) assay is not feasible in the presence of ATP. Since ATP shares the final stages of the degradation pathway with guanine nucleotides (see Figure 1), breakdown of ATP would also contribute to the colour production.

The first (HPLC) assay would be more amenable to this analysis since one could include ATP with the addition of GMP. The problem again lies in the shared components of the pathway – the production of catabolites past guanine could not be meaningfully monitored. It may therefore be necessary to design an assay in which radiolabeled GMP is used. The label could then be followed through the entire pathway, and non-labeled ATP degradation products would not interfere.

Summary

Inbred mouse strains were found to vary in erythrocytic GTP levels by as much as 16-fold. Based on their GTP levels, inbred strains were found to segregate into two distinct groups: those with low GTP and those with high GTP. ATP levels, on the other hand, were not found to differ significantly.

Regardless of the amount of GTP observed, all mice were phenotypically normal. This may be due to the fact that GTP levels in other cells remain constant across strains, suggesting that the observed GTP variations are a result of the differentiated state of the erythrocyte.

Erythrocytic GTP levels were found previously to be governed by the GTP concentration determining trait (*Gtpc*) located on mouse chromosome 9 (Jenuth *et al.* 1994). Over 200 mice were typed in this study for GTP concentrations and eight microsatellite markers to refine the map position of the *Gtpc* locus. The following order and map distances (in cM±S.E.) were obtained: (*D9Mit14*) 0.4±0.4 (*D9Mit24*) 1.7±0.8 (*Gtpc, D9Mit51, D9Mit116, D9Mit212*) 3.9±1.3 (*D9Mit200*) 3.0±1.1(*D9Mit20*) 7.8±1.8 (*D9Mit18*). These eight markers were also mapped in four recombinant inbred strain sets to continue to characterize this sub-region of chromosome 9.

A preliminary study of GTP catabolism suggests that an enzyme involved in GMP breakdown may be the source of the erythrocytic GTP variations observed.

Finally, from these experiments has come a large accumulation of tissues obtained from [(B6XWB)F_1XB6] backcross offspring. In addition to being useful in the present study, this store represents a valuable resource for future mapping studies involving inbred laboratory strains.

In conclusion, it is anticipated that complete characterization of GTP concentration variability in the mouse, including identification of the gene product involved in determining GTP levels, will lead to a better understanding of the regulation of purine metabolism. This may in turn provide greater insight into a number of neurological disorders that are known to be associated with reduced erythrocyte GTP levels, or impaired utilization of GTP.

References

BAILEY, D. W., 1971 Recombinant inbred strains. Transplantation **11:** 325-327.

BARANOV, V. S., SCHWARTZMAN, A. L., GORBUNOVA, V. N., GAITSKHOKI, V. S., RUBTSOV, N. B., TIMCHENKO, N. A., and S. A. NEIFAKH, 1987 Chromosomal localization of ceruloplasmin and transferrin genes in laboratory rats, mice and in man by hybridization with specific DNA probes. Chromosoma **96:** 60-66.

BIDDLE, F. G., COFFARO, C. M., ZIEHR, J. E., and B. A. EALES, 1993 Genetic variation in paw preference (handedness) in the mouse. Genome **36:** 935-943.

BIDDLE, F. G., and B. A. EALES, 1996 The degree of lateralization of paw usage (handedness) in the mouse is defined by three major phenotypes. Behav. Genet. **26:** 391-406.

BLATT, C., EVERSOLE-CIRE, P., COHN, V. H. ZOLLMAN, S., FOURNIER, R. E. K., MOHANDAS, L. T., NESBITT, M., LUGO, T., JONES, D. T., REED, R. R., WEINER, L. P., SPARKES, R. S., and M. I. SIMON, 1988 Chromosomal localization of genes encoding guanine nucleotide-binding protein subunits in mouse and human. Genetics **85:** 7642-7646.

BØTKER, H. E., KIMOSE, H. H., HELLIGSØ, P., and T. T. NIELSEN, 1994 Analytical evaluation of high energy phosphate determination by high performance liquid chromatography in myocardial tissue. J. Mol. Cell. Cardiol. **26:** 41-48.

BOURNE, H. R., SANDERS, D. A., and F. MCCORMICK, 1990 The GTPase superfamily: a conserved switch for diverse cell functions. Nature **348:** 125-132.

BOURNE, H. R., SANDERS, D. A., and F. MCCORMICK, 1991 The GTPase superfamily: conserved structure and molecular mechanism. Nature **349:** 117-127.

BRADFORD, M. M., 1976 A rapid and sensitive method for the quantitation of microgram quantities of protein utilizing the principle of protein-dye binding. Anal. Biochem. **72:** 248.

CHAPMAN, V. M., KRATZER, P. G., and B. A. QUARANTILLO, 1983 Electrophoretic variation for X chromosome-linked hypoxanthine phosphoribosyl transferase (HPRT) in wild-derived mice. Genetics **103:** 785-795.

CHEAH, Y. C., NADEAU, J. H., PUGH, S., and B. PAIGEN, 1994 New murine polymorphisms detected by random amplified polymorphic DNA (RAPD) PCR and mapped by use of recombinant inbred strains. Mamm. Genome **5:** 762-767.

CHILDS, K. F., NING, X.-H., and S. F. BOLLING, 1996 Simultaneous detection of nucleotides, nucleosides and oxidative metabolites in myocardial biopsies. J. Chromatogr. B **678:** 181-186.

COPELAND, N. G., JENKINS, N. A., GILBERT, D. J., EPPIG, J. T., MALTAIS, L. J., MILLER, J. C., DIETRICH, W. F., WEAVER, A., LINCOLN, S. E., STEEN, R., G. 1993 A genetic linkage map of the mouse: Current applications and future prospects. Science **262:** 57-66.

CROSS, D. R., MILLER, B. J., and S. J. JAMES, 1993 A simplified HPLC method for simultaneously quantifying ribonucleotides and deoxyribonucleotides in cell extracts or frozen tissues. Cell Prolif. **26:** 327-336.

CUNLIFFE-BEAMER, T. L., 1983 Biomethodology and surgical techniques, pp. 401-437 in *The Mouse in Biomedical Research Vol. III*, edited by H. L. Foster, J. D. Small, and J. G. Fox. Academic Press, New York.

DEAN, B. M., PERRETT, D., and M. SENSI, 1978 Changes in nucleotide concentrations in the erythrocytes of man, rabbit and rat during short-term storage. Biochem. Biophys. Res. Comm. **80:** 147-154.

DEMMER, L. A., BIRKENMEIER, E. H., SWEETSER, D. A., LEVIN, M. S., ZOLLMAN, S. SPARKES, R. S., MOHANDAS, T., LUSIS, A. J., and J. I. GORDON, 1987 The cellular retinol binding protein II gene. Sequence analysis of the rat gene, chromosomal localization in mice and humans, and documentation of its close linkage to the cellular retinol binding protein gene. J. Biol. Chem. **262:** 2458-2567.

DIETRICH, W., KATZ, H., LINCOLN, S. E., SHIN, H. S., FRIEDMAN, J., DRACOPOLI, N. C., and E. S. LANDER, 1992 A genetic map of the mouse suitable for typing intraspecific crosses. Genetics **131:** 423-447.

DIETRICH, W. F., MILLER, J. C., STEEN, R. G., MERCHANT, M. DAMRON, D., NAHF, R., GROSS, A., JOYCE, D. C., WESSEL, M., DREDGE, R. D., MARQUIS, A., STEIN, L. D., GOODMAN, N., PAGE, D. C., and E. S. LANDER, 1994 A genetic map of the mouse with 4,006 simple sequence length polymorphisms. Nature Genet. **7:** 220-225.

DRIVAS, G., MASSEY, R., CHANG, H. Y., RUSH, M. G., and P. D'EUSTACHIO, 1991 *Ras*-like genes and gene families in the mouse. Mamm. Genome **1:** 112-117.

EICHER, E. M., and E. P. SHOWN, 1993 Molecular markers that define the distal ends of mouse autosomes 4, 13, 19 and the sex chromosomes. Mamm. Genome **4:** 226-229.

ELLIOT, R. W., 1979 Mouse variants studied by two-dimensional electrophoresis. Mouse News Lett. **61:** 59.

ELLIOT, R. W., HOHMAN, C., ROMIJKO, C., LOUIS, P., and F. LILLY, 1978 Use of High resolution two dimensional electrophoresis of liver cytosol proteins in the discovery and mapping of a new mouse variant. pp. 261-274 in *Electrophoresis*, edited by N. Catsimpoolas. Elsevier North Holland, Amsterdam.

ELLIOT, R. W., and C. H. YEN, 1991 DNA variants with telomere probe enable genetic mapping of ends of mouse chromosomes. Mamm. Genome **1:** 118-122.

FRANKEL, W. N., and J. M. COFFIN, 1994 Endogenous nonecotropic proviruses mapped with oligonucleotide probes from the long terminal repeat region. Mamm. Genome **5:** 275-281. [published erratum appears in Mamm. Genome **5:** 463 (1994)]

FRIEDMAN, J. M., SCHNEIDER, B. S., BARTON, D. E., and U. FRANCKE, 1989 Level of expression and chromosome mapping of the mouse cholecystokinin gene: implications for murine models of genetic obesity. Genomics **5:** 463-469.

GLESNE, D. A., COLLART, F. R., and E. HUBERMAN, 1991 Regulation of IMP dehydrogenase gene expression by its end products, guanine nucleotides. Mol. Cell. Biol. **11:** 5417-5425.

GLESNE, D., COLLART, F., VARKONY, T., DRABKIN, H., and E., HUBERMAN, 1993 Chromosomal localization and structure of the human type II IMP dehydrogenase gene (IMPDH2). Genomics **16:** 274-277.

GREEN, E. L. 1981 *Genetics and Probability in Animal Breeding Experiments.* Oxford University Press, New York.

GRUBER, H. E., JANSEN, I., WILLIS, R. C., and J. E. SEEGMILLER, 1985 Alterations of inosinate branchpoint enzymes in cultured human lymphoblasts. Biochim. Biophys. Acta **846:** 135-144.

HALDANE, J. B. S., and C. H. WADDINGTON, 1931 Inbreeding and linkage. Genetics **16:** 357-374.

HENDERSON, J. F., ZOMBOR, G., JOHNSON, M. M., and C. M. SMITH, 1983 Variation in erythrocyte purine metabolism among mouse strains. Comp. Biochem. Physiol. B Comp. Biochem. **76:** 419-422.

HODGES, S. D., FUNG, E., MCKAY, D. J., RENAUX, B. S., and F. F. SNYDER, 1989 Increased activity, amount, and altered kinetic properties of IMP dehydrogenase from mycophenolic acid-resistant neuroblastoma cells. J. Biol. Chem. **264:** 18137-18141.

ICHINOSE, H., OHYE, T., TAKAHASHI, E., SEKI, N., HORI, T., SEGAWA, M., NOMURA, Y., ENDO, K., TANAKA, H., TSUJI, S., FUJITA, K., and T. NAGATSU, 1994 Hereditary progressive dystonia with marked diurnal fluctuations caused by mutations in the GTP cyclohydrolase I gene. Nature Genetics **8:** 236-242.

ICHINOSE, H., OHYE, T., MATSUDA, Y., HORI, T., BLAU, N., BURLINA, A., ROUSE, B., MATALON, R., FUJITA, K., and T. NAGATSU, 1995 Characterization of mouse and human GTP cyclohydrolase I genes. Mutations in patients with GTP cyclohydrolase I deficiency. J. Biol. Chem. 1995: 10062-10071.

ITOH, R., 1981 Purification and some properties of cytosol 5'-nucleotidase from rat liver. Biochim. Biophys. Acta **657:** 402-410.

JENKINS, N. A., COPELAND, N. G., TAYLOR, B. A., BEDIGIAN, H. G., and B. K. LEE, 1982 Ecotropic murine leukemia virus DNA content of normal and lymphomatous tissues of BXH-2 recombinant inbred mice. J. Virol. **42:** 379-388.

JENUTH, J. P., DILAY, J. E., FUNG, E., MABLY, E. R., and F. F. SNYDER, 1991 Absence of dGTP accumulation and compensatory loss of deoxyguanosine kinase in purine nucleoside phosphorylase deficient mice. pp. 273-276 in *Purine Metabolism in Man VII, Part B*, edited by R. A. Harkness, G. B. Elion, and N. Zöllner. Plenum Press, New York.

JENUTH, J. P., FUNG, E., and F. F. SNYDER, 1994 Assignment of a gene that determines erythrocytic guanosine-5'-triphosphate concentration (*Gtpc*) to mouse chromosome 9. Genome **37:** 399-404.

JINNAH, H. A., PAGE, T., and T. FRIEDMANN, 1993 Brain purines in a genetic mouse model of Lesch-Nyhan Disease. J. Neurochem. **60:** 2036-2045.

KINGSLEY, D. M. 1993 Mouse chromosome 9. Mamm. Genome **4:** S136-S153.

KUEHN, M. R., BRADLEY, A., ROBERTSON, E. J., and M. J. EVANS, 1987 A potential animal model for Lesch-Nyhan syndrome through introduction of HPRT mutations into mice. Nature **326:** 295-298.

LAIRD, P. W., ZIJERVELD, A., LINDERS, K., RUDNICKI, M., JAENISCH, R., and A. BERNS, 1991 Simplified mammalian DNA isolation procedure. Nucleic Acids Res. **19:** 4293-4296.

LALLEY, P. A., NAYLOR, S. L., ELLIOTT, R. W., and T. B. SHOWS, 1982 Assignment of *Acy-1* to mouse Chromosome 9: evidence for homologous linkage groups in man and mouse. Cytogenet. Cell Genet. **32:** 293.

LANDAW, S. A., and H. S. WINCHELL, 1970 Endogenous production of ^{14}CO: a method for calculation of RBC life-span *in vivo*. Blood **36:** 642-671.

MABLY, E. R., FUNG, E., and F. F. SNYDER, 1989 Genetic deficiency of purine nucleoside phosphorylase in the mouse. Characterization of partially and severely enzyme deficient mutants. Genome **32:** 1026-1032.

MANLEY, K. F. , and R. W. ELLIOT, 1991 RI Manager, a micro computer program for analysis of data from recombinant inbred strains. Mamm. Genome **1:** 123-126.

MEISLER, M. H., 1976 Effects of the *Bgs* locus on mouse beta-galactosidase. Biochem. Genet. **14:** 921-932.

MILTON J. S., 1992 *Statistical Methods in the Biological and Health Sciences. Second Edition.* McGraw-Hill, Inc., New York.

MIT CENTER FOR GENOME RESEARCH, July 1997 The Whitehead Institute for Biomedical Research, Cambridge, Massachusetts. World Wide Web (URL: http://www.genome.wi.mit.edu/)

MOUSE GENOME DATABASE (MGD), July 1997 Mouse Genome Informatics, The Jackson Laboratory, Bar Harbor, Maine. World Wide Web (URL: http://www.informatics.jax.org/).

MU, J. L., CHEAH, Y. C., and B. PAIGEN, 1992 Strain distribution pattern of 25 simple sequence length polymorphisms in the AXB and BXA recombinant inbred strains. Mamm. Genome **3:** 705-708.

NADEAU, J. H., DAVISSON, M. T., DOOLITTLE, D. P., GRANT, P., HILLYARD, A. L., KOSOWSKY, M. R., and T. H. RODERICK, 1992 Comparative map for mice and humans. Mamm. Genome **3:** 480-536.

NADEAU, J. H., KOMPF, J., SIEBERT, G., and B. A. TAYLOR, 1981 Linkage of *Pgm-3* in the house mouse and homologies of three phosphoglucomutase loci in mouse and man. Biochem. Genet. **19:** 465-474.

NAGGERT, J. K., SVENSON, K. L., LIN, L., CHEAH, Y. C., NISHINA, P. M., MU, J. L., DEVEREUX, T. R., YOU, M., and B. PAIGEN, 1997 An additional 136 SSLP markers typed for the AXB and BXA recombinant inbred mouse strains. Mamm. Genome **8:** 209-211.

NASS, S. J., OLOWSON, M., MIYASHITA, N., MORIWAKI, K., BALLING, R., and K. IMAI, 1993 Mapping of the *Mod-1* locus on mouse chromosome 9. Mamm. Genome **4:** 333-337.

NICHOL, C. A, SMITH, G. K., and D. S. DUCH, 1985 Biosynthesis and metabolism of tetrahydrobiopterin and molybdopterin. Ann. Rev. Biochem. **54:** 729-764.

PERRETT, D., and T. GRUNE, 1994 Rapid simultaneous measurement of nucleotides, nucleosides and bases in tissues by capillary electrophoreses. *Poster presented at the* Eighth International Symposium on Purine and Pyrimidine Metabolism in Man, Bloomington, Indiana.

RUSSELL, E. S., NEUFELD, E. F., and C. T. HIGGINS, 1951 Comparison of normal blood picture of young adults from 18 inbred strains of mice. Proc. Soc. Exp. Biol. Med. **78:** 761-766.

SEEGMILLER, J. E., ROSENBLOOM, F. M., and W. N. KELLEY, 1967 Enzyme defect associated with a sex-linked human neurological disorder and excessive purine synthesis. Science **155:** 1682-1684.

SHERLEY, J. L., 1991 Guanine nucleotide biosynthesis is regulated by the cellular p53 concentration. J. Biol. Chem. **266:** 24815-24828.

SIMMONDS, H. A., WATSON, A. R., WEBSTER, D. R., SAHOTA, A., and D. PERRETT, 1982 GTP depletion and other erythrocyte abnormalities in inherited PNP deficiency. Biochem. Pharmacol. **31:** 941-946.

SIMMONDS, H. A., FAIRBANKS, L. D., MORRIS, G. S., MORGAN, G., WATSON, A. R., TIMMS, P., and B. SINGH, 1987 Central nervous system dysfunction and erythrocyte guanosine triphosphate depletion in purine nucleoside phosphorylase deficiency. Arch. Dis. Child. **62:** 385-391.

SIMMONDS, H. A., FAIRBANKS, L. D., MORRIS, G. S., WEBSTER, D. R., and E. H. HARLEY, 1988 Altered erythrocyte nucleotide patterns are characteristic of inherited disorders of purine or pyrimidine metabolism. Clin. Chim. Acta **171:** 197-210.

SNYDER, F. F., and J. F. HENDERSON, 1973 A kinetic analysis of purine nucleotide synthesis and interconversion in Ehrlich ascites tumor cells *in vitro*. J. Cell. Physiol. **82:** 349-362.

SNYDER, F. F., JENUTH, J. P., DILAY, J. E., FUNG, E., LIGHTFOOT, T., and E. R. MABLY, 1994 Secondary loss of deoxyguanosine kinase activity in purine nucleoside phosphorylase deficient mice. Biochim. Biophys. Acta **1227:** 33-40.

SNYDER, F. F., JENUTH, J. P., NOY, J. L., WIEBE, G., and E. FUNG, 1994 Mapping a gene that determines erythrocytic GTP concentration to a region of mouse chromosome 9 which is syntenic to human chromosome 3p. (Abstract) Am. J. Hum. Genet. **55:** A204.

SOKAL, R. R., and F. J. ROHLF, 1969 *Biometry.* W. H. Freeman and Co., New York.

SOKAL, R. R., and F. J. ROHLF, 1981 *Biometry. Second Edition.* W. H. Freeman and Co., New York.

TAYLOR, B. A., and P. C. REIFSNYDER, 1993 Typing recombinant inbred mouse strains for microsatellite markers. Mamm. Genome **4:** 239-242.

TORRES, R. J., MATEOS, F. A., PUIG, J. C. and M. A. BECKER, 1994 A simplified method for the determination of phosphoribolsylpyrophosphate synthetase activity in hemolysates. Clin. Chim. Acta **224:** 55-63.

VAGLIANI, M., MELANI, C., PARMIANI, G., D'EUSTACHIO, P., WETTSTEIN, P. J., and M. P. COLOMBO, 1993 Immunodominance in the T-cell response to multiple non-H-2 histocompatibility antigens. V. Chromosomal mapping of the immunodominant cytotoxic T-cell target-1 (CTT-1). Immunogenetics **38:** 157-160.

VAN DEN BERGHE, G., VAN POTTELSBERGHE, C. and H.-G. HERS, 1977 A kinetic study of the soluble 5'-nucleotidase of rat liver. Biochem. J. **162:** 611-616.

WILLIS, R. C., and J. E. SEEGMILLER, 1980 Increases in purine excretion and rates of synthesis by drugs inhibiting IMP dehydrogenase or adenylosuccinate synthase activities. pp. 237-241 in *Purine Metabolism in Man. III. Biochemical, Immunological and Cancer Research*, edited by A. Rapado, R.W.E. Watts, and C.H.M.M. DeBruyn. Plenum Publishing Corporation, New York.

WOMACK, J. E., DAVISSON, M. T., EICHER, E. M., and D. M. KENDALL, 1977 Mapping of nucleoside phosphorylase (*Np-1*) and esterase10 (*Es-10*) on mouse chromosome 14. Biochem. Genet. **15:** 347-355.

WOODWARD, S. R., SUDWEEKS, J., and C. TEUSCHER, 1992 Random sequence oligonucleotide primers detect polymorphic DNA products which segregate in inbred strains of mice. Mamm. Genome **3:** 73-78.

YOUNGBLOOD, G. L., NESBITT, M. N., and A. H. PAYNE, 1989 The structural genes encoding P450scc and P450arom are closely linked on mouse chromosome 9. Endocrinology **125:** 2784-2786.

APPENDIX

Human Erythrocytic Nucleotide Concentrations

Human blood was analyzed to determine whether erythrocytic GTP levels vary significantly within the population. Ethical approval was obtained to use remnant blood taken for a study unrelated to this thesis. Nucleotides were extracted from blood samples using the same methods employed for mouse samples. Unfortunately, because these were remnant samples, the time from when the blood was drawn until the nucleotides were extracted varied widely. Therefore, the extraction efficiency was considerably variable, as indicated by the wide range of ATP/ADP ratios (3.9 - 13.2).

Twenty-four different individuals were sampled for this study: thirteen males and eleven females. A complete nucleotide profile is presented for future consideration (Table 15). The GTP/ATP ($x10^2$) ratio obtained (4.3 ± 0.7) in this study is comparable to the ratio 4.2 reported by Simmonds *et al.* (1988). The GTP/ATP ($x10^2$) ratio is not significantly different between males (4.0 ± 0.7) and females (4.5 ± 0.6) based on a 95% confidence interval (Milton 1992). Because humans are a largely heterogeneous group, it was expected that levels would indicate a continuum, rather than distinct groupings of GTP and ATP levels, as

observed in mice. Rankit plot analysis confirms this (Figure 16), and shows no significant variations in GTP concentrations. In fact, human erythrocytic GTP/ATP ($x10^2$) varies little (3.0 - 5.2); the standard error is comparable to that of a single given mouse strain.

It should be noted that the blood samples used in this experiment do not represent a random cross-section of the population. Rather, they are taken from research personnel within the facility, who are predominantly from European backgrounds. Therefore, the results found in this study may not be representative of the entire human population.

An unexpected peak was found in the HPLC absorbance spectrum of eight (five males, three females) of the 24 individuals sampled. It is an extremely large peak (see Figure 17) with a retention time of 12.0 minutes, and an absorbance maximum of 238 nm. It elutes close to IMP (which has a retention time of 12.8 minutes) thus obscuring the typically small IMP peak. The identity of this peak is still being investigated. Tryptophan, tyrosine phenylalanine and histidine, which absorb in the ultra-violet range, will be considered. Caffeine and methyl-xanthines have been ruled out as possible candidates (based on retention times and absorbance spectra). It would be informative to take samples from these individuals over time, to determine whether this peak is constant, or

transient. If the latter, that may suggest that it has a dietary source, which could be followed by monitoring corresponding food intake.

Table 15. Human erythrocytic nucleotide concentrations.

Nucleotide	Concentration (nmol/mL packed cells)	Number*
NAD^+	48 ± 11	n=24
IMP	4 ± 4	n=16***
UDP-hexose	16 ± 10	n=14**
UDP	61 ± 13	n=24
UTP	2	n=1
CDP	3 ± 1	n=12
CTP	17 ± 8	n=15
GMP	15 ± 5	n=14**
GDP	6 ± 1	n=24
GTP	41 ± 8	n=24
AMP	13 ± 13	n=24
ADP	125 ± 47	n=24
ATP	967 ± 140	n=24
GTP/ATP $x10^2$	4.3 ± 0.7	N/A
ATP/ADP	8.5 ± 2.4	N/A
peak 238 nm	N/A	n=8***

* refers to the number of individuals of the total 24 sampled who are exhibiting the corresponding peak in the HPLC spectra.

**GMP and UDP-hexose are often co-eluting

*** large unidentified peak with absorbance max. at 238 nm obscures IMP peak

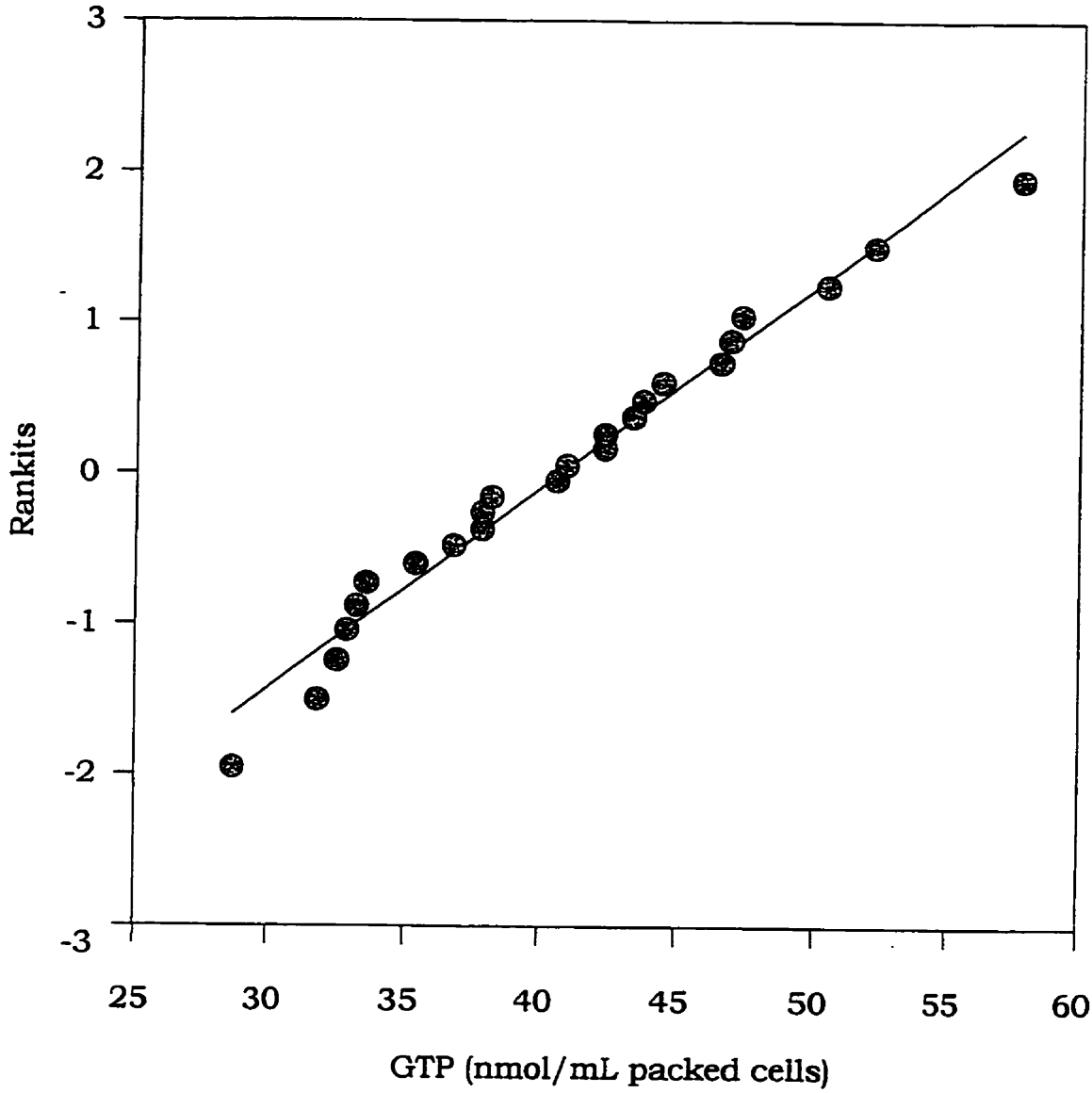

Figure 16. Rankit analysis (Sokal & Rohlf 1981) of human erythrocytic GTP concentrations. Each circle represents one individual. A first order regression line is fitted to the data.

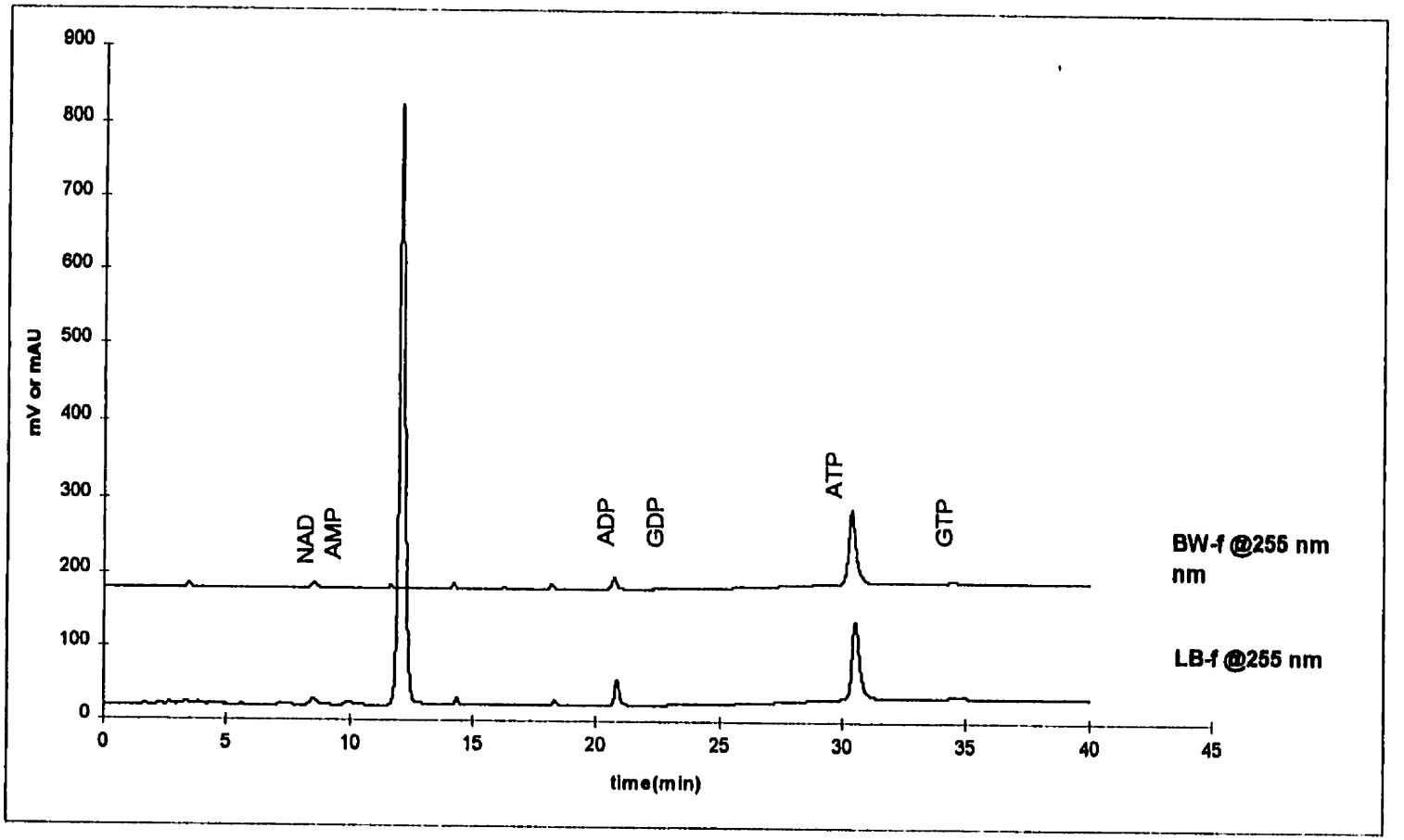

Figure 17. HPLC analysis of human erythrocytic nucleotides. Note the presence of the peak which elutes at 12 minutes in sample LB-f but not BW-f.

TEST TARGET (QA-3)

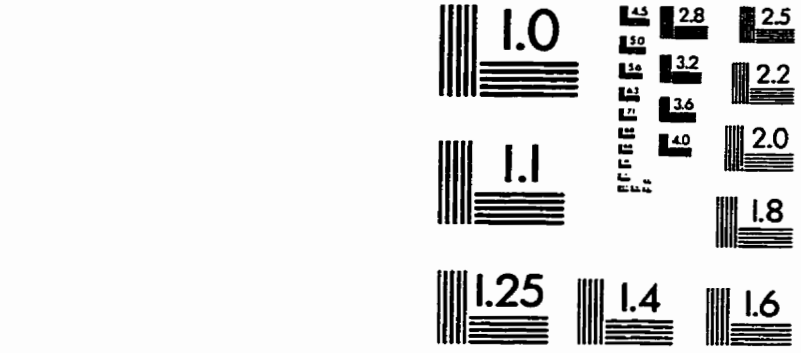

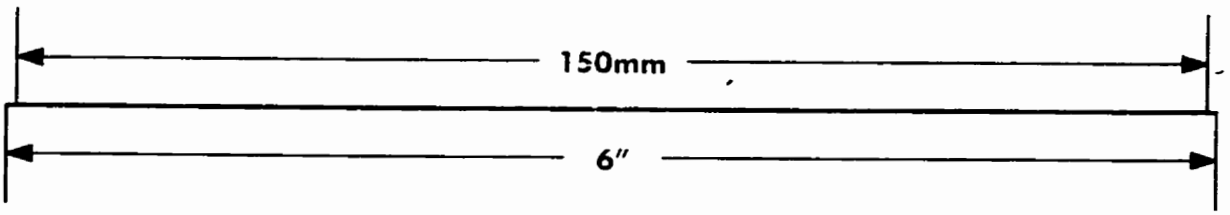

APPLIED IMAGE, Inc
1653 East Main Street
Rochester, NY 14609 USA
Phone: 716/482-0300
Fax: 716/288-5989